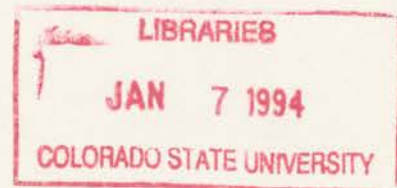


AFOSR Grant 91-0269

PROTOTYPE TERMINAL AERODROME FORECASTS
USING A MESOSCALE MODEL

by Capt. Benjamin I. Edwards, II



William R. Cotton, P.I.

**Colorado
State
University**

**DEPARTMENT OF
ATMOSPHERIC SCIENCE**

PAPER NO. 544

PROTOTYPE TERMINAL AERODROME FORECASTS
USING A MESOSCALE MODEL

by

Capt. Benjamin I. Edwards, II
Department of Atmospheric Science
Colorado State University
Fort Collins, CO 80523

Research Supported by

Air Force Office of Scientific Research
under Grant 91-0269

December 14, 1993

Atmospheric Science Paper No. 544



U18401 0105072

QC
852
.Cl
NO. 544
ATSL

ABSTRACT

PROTOTYPE TERMINAL AERODROME FORECASTS USING A MESOSCALE MODEL

The purpose of this study is to evaluate the potential of the Regional Atmospheric Modeling System (RAMS) in this configuration to forecast convective cloud coverage, timing, location, and precipitation on a mesoscale grid. Using this model output a prototype terminal aerodrome forecast (TAF) has been produced. RAMS was developed at Colorado State University and is being used to simulate convection over central Florida using a nested grid model where the smallest grid had a horizontal spacing of 5 kilometers. To obtain meaningful results a 2.5w cumulus parameterization scheme was used. The traditional cumulus parameterization schemes assume that the effect of convection is limited to one grid box, this assumption does not apply on grid spacings of 5 kilometers.

The model was evaluated using data collected by the Convection and Precipitation Electrification Experiment (CaPE) over Florida during the summer of 1991. The model performed a 12 hour forecast valid from 12Z on 29 July 1991 to 00Z on 30 July. The course grid had a horizontal grid spacing of 80 kilometers and covered an area from Washington D.C. south to the western edge of Hispanola and west to Fort Worth Texas and north to Topeka Kansas. This area includes most of the Gulf of Mexico and extends 200 kilometers east of Cape Hatteras North Carolina. The second grid has a horizontal grid spacing of 20 kilometers and covers the Florida peninsula and adjacent coastal waters. The third grid was centered over the Kennedy Space Center Florida and is approximately 40 kilometers north, west, and south and 20 kilometers east over the ocean.

The placement and size of the third grid was used to evaluate the usefulness of a producing model-aided TAF's. One of the problems facing the forecasting community is

how to prepare a TAF, the aviation communities forecast, with the current NWP products. Currently forecasters use the Nested Grid Model (NGM) with a horizontal grid spacing of 80 kilometers. The resolution of the NGM is 320 kilometers and is totally inadequate for the task of preparing an aviation forecast. Aviation forecasts are valid for the weather within 20 kilometers of the runway. The NGM parameterizes convection on this scale while the 2.5w parameterization can explicitly resolve features on the 5 kilometer scale. This increased resolution will greatly aid in the production of aviation forecast. As a demonstration the RAMS model output will be used to produce a TAF for Kennedy Space Center.

Capt. Benjamin I. Edwards, II
Department of Atmospheric Science
Colorado State University
Fort Collins, Colorado 80523
Fall 1993

ACKNOWLEDGEMENTS

First I would like to thank my advisor, Dr. William Cotton, for allowing me the opportunity to pursue my degree under his tutelage. Dr. Cotton has taught me a great deal about atmospheric science and how to appreciate computer models. He was always there with a suggestion on where to go when I needed it. I would also like to thank my other committee members, Dr. Roger Pielke from the Atmospheric Science Department and Dr. Chandrasekar from the Electrical Engineering Department. I have to admit that I was leary of two modelers on my committee but their insights have proved extremely valuable.

I would like to thank the Air Force for allowing me the opportunity to pursue my education. I would especially like to thank Capt Robert Uland for recommending that I be accepted into the Air Force Institute of Technology program and Maj Mary Smith for overseeing my program of study. I am deeply indebted to the men and women of the weather detachment at Charleston AFB, South Carolina for taking a budding meteorologist and teaching me to forecast. The Air Force Office of Scientific Research purchased the computer on which the simulations were performed.

The support staff at CSU has been invaluable. A special thanks to Brenda Thompson for always knowing the right key stroke for the text editor, without whose help this thesis wouldn't look nearly as professional. I would like to extend my appreciation to Lucy McCall and Dallas McDonald for tracking down innumerable articles. My computer and I would like to thank Donna Chester for keeping computer operating and preventing me from committing fratricide. Drs. Bob Walko and Craig Tremback are thanked for their insights into the RAMS code. Dr. Mike Weissbluth is also thanked for developing the cumulus parameterization I used.

I would like to thank my office mate of the last two years, David Mocko. Thanks for restraining me when Donna wasn't around to protect the computer. We navigated

the RAMS code maze together, next time bring more magic missiles though. My deepest gratitude is also extended to all the RAMS users for answering my questions and providing some illumination in its dark recesses. Greg Thompson's help is especially appreciated, particularly the analysis package.

I would like to thank all those who have provided data to verify the model. Special thanks are due to Steve Finley at CSU. Steve Williams at NCAR and Bill Crosson at Marshall Space Flight Center provided data from the CaPE experiment.

The support at home has also been wonderful. I would like to thank my wife, Carmen, for tolerating me when the computer didn't. You have been exceptional taking care of our children while I wasn't there. I would also like to thank my children, Galen and Logan. You probably won't remember much of this assignment, but thanks for letting me go to work when all of us would rather be playing. A special thanks to Galen (age 4) for explaining where rain comes from - the clouds have too much water. Hopefully, I can explain it a little better.

I would also like to express my appreciation to the Air Force Office of Scientific Research. AFOSR grant 91-0269 provided administrative support and underwrote the cost of my research. I am deeply indebted to them for the computer these simulations were performed on.

I would also like to thank YHWH for all the help.

TABLE OF CONTENTS

1 INTRODUCTION TO MESOSCALE NUMERICAL PREDICTION	1
1.1 History	1
1.2 The Introduction of Computers	2
1.2.1 Synoptic-scale Models	2
1.2.2 Producing Model-Aided Forecasts	3
1.2.3 Mesoscale Models	4
1.2.4 Producing Model-Aided TAF's	5
2 MODEL DESCRIPTION	9
2.1 The ISAN package	9
2.2 The Model Package	10
2.2.1 Model Numerical Procedures	10
2.2.2 Boundary Conditions	11
2.2.3 Eddy Diffusion	12
2.2.4 Cumulus Parameterization	12
2.2.5 Microphysical Parameterization	15
2.2.6 Radiation Parameterization	15
2.2.7 Surface Parameters	16
2.2.8 Changes from the standard code	16
2.3 The VAN Package	17
2.4 The Domain	18
3 RESULTS OF THE RAMS SIMULATIONS	21
3.1 The Experiments	21
3.2 Synoptic Conditions	23
3.3 The Control Case	33
3.4 Changing the radiation simulation	53
4 PRODUCING AN AVIATION FORECAST	57
4.1 Producing Terminal Aerodrome Forecasts	57
5 CONCLUSIONS	63
6 FUTURE RESEARCH	64
6.1 Mesoscale models	64
6.2 RAMS	65

LIST OF FIGURES

2.1	Model Domain. Grids 1, 2, and 3	18
2.2	Grid 3 domain. Centered over the Kennedy Space Center	19
3.1	NMC analyzed surface chart; 12Z 29 July	24
3.2	Model initialized sea level pressure (mb); 12Z 29 July	24
3.3	Model sea level pressure (mb); 13Z 29 July	25
3.4	Model initialized 850 mb geopotential heights (m); 12Z 29 July	26
3.5	NMC analyzed 850 mb upper air analysis; 12Z 29 July	26
3.6	Model initialized 700 mb geopotential heights (m); 12Z 29 July	27
3.7	Model initialized 500 mb geopotential heights (m); 12Z 29 July	28
3.8	NMC analyzed 500 mb upper air analysis; 12Z 29 July	28
3.9	NGM initialized mslp (mb) and 1000/500 mb thickness (m) analysis ; 12Z 29 July	29
3.10	NGM initialized 700 mb relative humidity; 12Z 29 July	29
3.11	NGM initialized 500 mb vorticity; 12Z 29 July	30
3.12	NGM 12 hour forecast surface pressure (mb); 00Z 30 July	31
3.13	NGM 12 hour forecast 700 mb relative humidity; 00Z 30 July	31
3.14	NGM 12 hour forecast 700 mb vertical velocities (cm/s)and precipitation (in); 00Z 30 July	32
3.15	NGM 12 hour forecast 500 mb vorticity; 00Z 30 July	32
3.16	Sea level pressure (mb); 18Z 29 July	34
3.17	NMC surface chart; 18Z 29 July	34
3.18	Sea level pressure (mb); 18Z 29 July	35
3.19	Temperature (°C); 18Z 29 July	36
3.20	Temperature (°C); 18Z 29 July	36
3.21	Near surface streamlined wind direction; 18Z 29 July	37
3.22	Near surface wind speed (m/s); 18Z 29 July	38
3.23	Cloud water mixing ratio (g/g), elevation = 406 m, Contour interval = 1 E-5 g/g, maximum contour = 10 E-5 g/g; 18Z 29 July	39
3.24	Condensation mixing ratio (g/g), elevation = 7679 m contour = 1 E-5 g/g, maximum contour = 1 E-5 g/g; 18Z 29 July	39
3.25	NMC radar summary; 1635Z 29 July	40
3.26	Near surface streamlined wind field; 21Z 29 July	41
3.27	Near surface wind speeds (m/s); 21Z 29 July	42
3.28	Accumulated convective precipitation (mm), contours = 6 mm, maximum con- tour = 12 mm; 21Z 29 July	42
3.29	Accumulated convective precipitation (mm), contour = 6 mm, maximum contour = 12 mm; 21Z 29 July	43
3.30	Condensate mixing ratio (g/g), elevation = 48.6 m contour = 1 E-5 g/g, maxi- mum contour = 14 E-5 g/g; 21Z 29 July	44

3.31	Condensate mixing ratio (g/g), elevation = 48.6 m contour = 1 E-5 g/g, maximum contour = 39 E-5 g/g; 21Z 29 July	44
3.32	Condensate mixing ratio (g/g), elevation = 7679 m, contour = 1 E-5 g/g, maximum contour = 32 E-5 g/g; 21Z 29 July	45
3.33	Condensate mixing ratio (g/g), elevation = 7679 m, contour = 1E-5 g/g, maximum contour = 39 E-5 g/g; 21Z 29 July	45
3.34	NMC radar summary; 2135Z 29 July	46
3.35	Mean sea level pressure (mb); 00Z 30 July	47
3.36	Temperature (°C); 00Z 30 July	47
3.37	Near surface streamlined winds; 00Z 30 July	48
3.38	Near surface wind speeds (m/s); 00Z 30 July	49
3.39	Accumulated convective precipitation (mm), contour = 6 mm, maximum contour = 24 mm; 00Z 30 July	50
3.40	NMC precipitation summary (in); 12Z 30 July	50
3.41	Accumulated convective precipitation (mm), contour = 6 mm, maximum contour = 18 mm; 00Z 30 July	51
3.42	Accumulated convective precipitation (mm), contour = 6 mm, maximum contour = 24 mm; 00Z 30 July	52
3.43	NMC radar analysis; 0035Z 30 July	53
3.44	Condensate mixing ratio (g/g), elevation = 48.6 m, contour = 1 E-5 g/g, maximum contour = 39 E-5; 00Z 30 July	54
3.45	Mean sea level pressure (mb); 00Z 30 July	55
3.46	Accumulated convective precipitation (mm), contour = 6 mm, maximum contour = 48 mm; 00Z 30 July	56
3.47	Mixing condensation ratio (g/g), elevation=48.6 m, contour = 1 E-5 g/g, maximum contour = 7 E-5 g/g; 00Z 30 July	56
4.1	Condensation mixing ratio cross section (g/g), contour = 1 E-5 g/g, maximum contour = 39 g/g; 21Z 29 July	61
4.2	Condensation mixing ratio (g/g), contour = 1E -5 g/g, maximum contour = 39 E -5 g/g; 21Z 29 July	62

Chapter 1

INTRODUCTION TO MESOSCALE NUMERICAL PREDICTION

1.1 History

Our culture is permeated with references to the weather; both forecasting the weather and its effects. Very few forces touch as many people or cause as much concern as the weather. The Book of Job is one of the oldest pieces of literature in Western society and it records how the skies clear after the wind has swept them clean (37:21). This passage closely describes a cold frontal passage which causes the winds to blow and then the skies clear in the drier air behind the front. Almost all ancient cultures record a cataclysmic flood that covers the earth.

Man's knowledge of weather increased from these early observations. By the third century B.C.E. Aristotle had divided the weather into polar and equatorial regimes with descriptions of each (Thompson, et al. 1965). In the mid 1700's, Benjamin Franklin was performing his famous kite experiment and noticing the cyclonic nature of storm systems. At the same time across the Atlantic another writer was making climatological observations. Mother Goose (1986) noted that

As the days get longer
the storms get stronger.

More recently man has been able to predict the weather based on scientific principles instead of just climatological observations. L.F. Richardson was the first to attempt to predict the weather using numerical methods (Holton, 1979). In 1922 Richardson published his treatise *Weather Prediction by Numerical Process*. In the book Richardson described how to solve for the time tendency term in the differential equations governing the atmosphere. Richardson's equations included the terms describing the propagation of sound

waves. Because of the inclusion of sound waves, the equations give pressure changes an order of magnitude larger than observed. The equations also used unstable explicit operators. This early failure was thought to be due to bad initial data though. Little progress was made on obtaining initial data. This caused many researchers not to proceed with Richardson's theories (Holton, 1979).

1.2 The Introduction of Computers

1.2.1 Synoptic-scale Models

Even if Richardson simplified his equations he still faced another problem, number crunching resources. Richardson envisioned placing people in a large room and passing the results of the calculations to the next person or grid point. Richardson estimated that to produce global forecasts 64,000 people would be needed (Holton, 1979). While this may solve unemployment problems it will not produce a very efficient forecast. It was not until the advent of computers that another serious attempt at numerical weather prediction was made.

At the end of World War II several important factors came together to resume the quest for the accurate weather forecast. First was the introduction of computers which solved the problem of number crunching. Secondly, meteorology had progressed enough to allow another attempt with equations that filtered out the sound waves. Finally, forcing; the size of the aviation community had increased dramatically during the war. While weather impacts everyone, the aviation community is especially sensitive to its fickleness. Additionally, Americans found themselves with more time for recreational activities. In order to enjoy the time outside they needed better forecast to plan their activities.

Charney described a set of equations that filtered out the sound waves and avoided the problems encountered by Richardson. These equations were modified for a barotropic atmosphere and used for numerical forecasting. The first operational numerical forecast was performed in 1950 (Holton, 1979). Since that time many advances have been made on a number of problems associated with numerical weather prediction. Among these are better computers, a better understanding of the atmosphere, improvements in the initialization of the model, and better use of mathematical skills. Where Charney used a barotropic model

with several very simplifying assumptions; the Regional Atmospheric Modeling System, RAMS, uses a full set of primitive equations.

Since that first operational model many others have been tried with increasing levels of sophistication. The United States Weather Service has successively used a baroclinic model, the primitive equation model, then the Limited Fine Mesh, LFM, and finally the Nested Grid Model, NGM. The primitive equation model was upgraded to the LFM in 1972 (Junker et al., 1989). Originally the LFM used a horizontal grid spacing of 190.5 kilometers and six vertical levels. The NGM was introduced in 1985 (Hoke et al., 1989) with several improvements over the LFM. In addition to improvements in the model physics, the resolution was also improved. Sixteen vertical levels are used throughout the domain and the smallest nested grid has a horizontal grid spacing of approximately 80 kilometers. Each model improves its resolution, vertically and horizontally. The upgrades in the models have closely followed the development of the computers used to run them.

1.2.2 Producing Model-Aided Forecasts

The barotropic model forecasts the 500 mb heights and winds. This allows the placement of weather systems but not what is normally considered "weather" forecasting. There is no forecast of surface winds, precipitation, or clouds. The NGM produces forecasts of parameters that effect people; temperature, precipitation, and winds at the first model level which is approximately 35 mb above the surface (Hoke et al., 1989). Depending on the computer resources available to a forecast office the NGM outputs data valid every six hours and every 50 mb in the vertical. There is still a large number of facilities that only receive the standard eight panel facsimile chart, even if they have computer resources. With these plots you are limited to the surface sea level pressure, 1000-500 thickness, 700 mb relative humidity and heights, the 500 mb height and vorticity, and the 700 mb vertical velocity and surface precipitation. With these parameters forecasts of winds, precipitation amounts, temperature, pressure, mid-level clouds, frontal passage, and the phase of the precipitation may be made. Is this a good forecast though? This depends on your definition of a good forecast. If you want to go to the beach and the regional forecast is for a temperature of

30°C and it only reaches 28°C because the sea-breeze was inaccurately forecast you probably consider it a “good” forecast. Consider another problem though, you are flying a small aircraft sightseeing a group of islands. The flight weather brief states that cloud base will be at or above 3000 feet, approximately 1000 meters. You are approaching an island from upwind when you enter cloud base. The flight plan called for a visual flight rule flight, no cloud penetrations, but the pilot presses on thinking that you will exit the cloud soon. Assuming the weather forecast is correct you will clear the 2500 foot peak with no problem and have a spectacular view when the clouds break. Seconds later you impact the side of the mountain. The pilot was not flying at 3000 feet but 2400 feet. While the crash was caused by pilot error, weather contributed to the tragedy. The model used to predict the weather failed to detect the orographic clouds because the model resolution did not even detect an island. Your survivors do not consider this a “good” forecast. This example was chosen for a number of reasons, it shows limitations of large scale models and one of the potential problems. The question arises of how to solve these deficiencies.

1.2.3 Mesoscale Models

The first of these questions is how to minimize the limitations of large scale models. To detect sea-breezes or small scale topographical features the resolution of the model can be increased. The resolution chosen depends on the scale of the phenomena. A much coarser grid spacing may be chosen if the model is expected to detect cold air damming along the Appalachians than if the model is to resolve the valleys in the mountains and detect valley fogs. While it may be impractical at present to prepare a forecast using a 20 kilometer grid spacing on the entire United States it is very practical to use a 20 kilometer grid spacing in a regional mesoscale model.

The first issue to be resolved is the definition of mesoscale. Orlanski (1975) defines a meso- α phenomena as having a characteristic length between 2000 and 200 kilometers, meso- β having lengths between 200 and 20 kilometers and meso- γ between 20 and 2 kilometers. This classification scheme contradicts the original concept of mesoscale disturbances as noise on the synoptic-scale disturbances (Fujita, 1986). Orlanski's scale is large enough to include cyclones and anticyclones as mesoscale phenomena. Anthes used this definition in

his review of regional models (1983) which led him include both the LFM and NGM in his review. Fujita (1981) proposed another classification system which defines the meso- α region as being between 400 and 40 kilometers and the meso- β scale between 40 kilometers and 4 kilometers. In this thesis we will use Fujita's definition. Furthermore, the scale of primary interest is in the meso- β region which is less than 40 kilometers. To be classified as a mesoscale model the model should be able to resolve mesoscale phenomena. Since the resolution is approximately four times the grid increment this requires that the grid spacing be considerably less than 100 kilometers even for meso- α phenomena.

Some of the problems that remain with mesoscale models is how to parameterize the sub-grid scale interactions and in the handling of the boundary conditions (Anthes, 1983). One of the major advantages is the capability to increase the complexity of the model physics. For instance, RAMS can utilize a microphysical parameterization scheme that predicts cloud water, rain, ice crystals, snow and graupel/hail. Additional advantages are in the representation of surface fluxes and the increased resolution of the topography.

1.2.4 Producing Model-Aided TAF's

TAF is short for Terminal Aerodrome Forecast and differs from a general public forecast in many respects. The general public forecast usually is something like 'partly cloudy, high in the mid-70's and chance of afternoon thunderstorms'. This forecast is useful to most people, it includes information on what they need to wear and if they are going to get wet. This forecast does not include enough information for the aviation community. The forecast for aviators is the TAF and includes parameters that are important to the aviation community and include cloud height and amounts, visibility, wind speed and direction, precipitation, thunderstorms, icing, turbulence and pressure. Currently models for aviation forecasting are still in the development stage. There are very few mesoscale models that are capable of resolving features less than 100 kilometers and with sufficient vertical resolution to assist in producing a TAF. The NGM has a horizontal grid spacing of 80 kilometers (Hoke et al., 1989). This is wholly inadequate for resolving parameters required by the TAF. Aviation forecasts are valid within approximately 20 kilometers of the runway. The

NGM can not resolve features less than 320 kilometers. Another problem with aviation forecasting is determining the ceiling and visibility which the NGM does not forecast.

The MM4 model is run in a real-time mode at the Pennsylvania State University on an IBM 3090 mainframe computer. The finest grid spacing is 30 kilometer and can therefore resolve features on the order of 120 kilometers (Warner and Seaman, 1990). The lowest model level is 50 meters above ground level. At this resolution there is no distinction made between low stratus and fog. Additionally, there is no mention of any visibility forecast in the model description provided by Warner and Seaman(1990), although they are working on this problem. The cumulus parameterization scheme used is Anthes (1977) which is a Kuo-type scheme. On this grid spacing it is questionable whether the assumptions of the Kuo scheme are still valid. Warner and Seaman state that the reason they use a Kuo-type scheme is that "it is the most thoroughly tested and therefore best "choice"", or an old shoe fits better than a new one. The model is also formulated using the hydrostatic assumption.

The United Kingdom Meteorological Office (UKMO) mesoscale model has a fine grid increment of 15 kilometers. This allows the model to resolve features larger than 60 kilometers. This is especially important in Great Britain where the local topography varies dramatically (Golding, 1990). The model dynamics are based on non-hydrostatic equations. The first model level is 10 meters above ground level but the second is 110 meters. Visibility forecast are made with this model. The model, however, can not distinguish between fog or low clouds (Golding, 1990). The model has recently been upgraded from 16 to 32 vertical levels (Golding, 1992) but results of the increased resolution are still not available. The British have opted to use the Fritsch-Chappel cumulus parameterization scheme. This assumes an ensemble of clouds and may not be appropriate on a scale of 15 kilometers. The Fritsch-Chappel scheme also requires that the clouds and their subsidence be confined to the same grid.

Colorado State has also entered the realm of real time forecasting. Thompson (1993) used RAMS to produce real time forecasts for Colorado during the winter season of 1991-1992. The fine grid used in Thompson's study was 25 kilometers. The model was initialized using data from the Mesoscale Analysis and Prediction System, MAPS. Even though MAPS

is a forecasting model only the initial fields were used by Thompson. The boundary conditions were specified by the NGM forecast and 48 hour predictions were made on a Stardent work station. Work is continuing to produce real time forecast for convective events during the spring and summer of 93 with a fine grid of 16 kilometers. The model uses primitive equations with a non-hydrostatic compressible equation of motion. The cumulus scheme currently used is a Kuo-type that has been modified by Tremback (1990).

The NOAA Forecast System Laboratory, FSL, is actually developing models designed to assist in producing TAF's. FSL is in the process of testing several of these models (Cairns, 1993). One of the models is MAPS. MAPS is run in a three hour cycle similar to the UKMO model. The model has a 60 kilometer grid spacing and can ingest data from a multitude of sources; standard observations, upper air data, profiler data, and aircraft reports or ACARS (Thompson, 1993). The version currently used has 25 levels in the vertical and uses a hybrid vertical isentropic- σ_z coordinate (Cairns, 1993). The low-level vertical coordinate is based on σ_z coordinates while the upper level coordinates are isentropic. In addition to predicting the standard atmospheric variables MAPS also predicts visibility, obstruction to visibility, ceiling, cloud heights, cloud amount and cloud top.

FSL is also testing a version of RAMS in four different regions of the United States to assist in aviation forecasting. One of the versions FSL is using is very similar to the one presented in this thesis. The RAMS configuration used by FSL in Florida has a 20 kilometer large grid and a 5 kilometer nested grid. The large grid only covers the Florida peninsula and the eastern Gulf of Mexico. The RAMS grid points have been rotated to allow the model to be initialized with the MAPS initialization data. RAMS uses 38 levels in the vertical with a σ_z vertical coordinate. The cumulus scheme is based on Weissbluth's (1991) work at CSU (see chapter 2 for a more complete description). RAMS forecasts the same variables as MAPS except it does not forecast visibility, obstruction to visibility, or cloud amount.

FSL is using an IBM RS6000/580 to perform the RAMS simulations. As discussed by Cotton et al. (1994) this is the next step in meteorological forecasting, moving away from a large national forecast requiring supercomputers, to regional models performed on work stations. RAMS is one such model. By judiciously choosing the grid and the various

dynamical and thermodynamical options a regional forecast can be produced. Furthermore, RAMS may be used to assist in preparing Terminal Aerodrome Forecast for the aviation community. In Chapter 2 we will examine some of the various options chosen for these simulations. Chapter 3 will deal with the model results. The discussion and forecast will follow in Chapter 4 while the conclusions will be discussed in Chapter 5. Future research for RAMS and mesoscale numerical prediction will be discussed in Chapter 6.

Chapter 2

MODEL DESCRIPTION

For these simulations the RAMS code locally known as version new 2c was used. The RAMS code has been developed at CSU as a comprehensive meteorological model that combined features from several earlier codes (Pielke, et al., 1992). The new 2c code features a hydrostatic mesoscale model (Mahrer and Pielke, 1977) and a non-hydrostatic cloud model (Tripoli and Cotton, 1982). General descriptions of the model code may be found in Cotton et al. (1982, 1986), Tripoli and Cotton (1982), Tremback et al. (1986), Tripoli (1986), Tremback (1990), Pielke et al. (1992) and Nicholls et al. (1993).

Any meteorological computer simulation consist of three distinct processes; initialization, simulation, and post-processing. These processes correspond to the ISentropic ANalysis, ISAN, the model, and the Visualization and ANalysis, VAN, packages of RAMS.

2.1 The ISAN package

The purpose of the ISAN package is to prepare a model-compatible field of observations. The code can use data sets provided by NMC rawinsonde, surface observations, and mandatory-level global analysis data. The code may also use either the ECMWF global analysis or the NOAA Forecast Systems Laboratory Mesoscale Analysis and Prediction System (MAPS) data sets (Pielke et al., 1992). The MAPS data set has a much finer resolution than either of the global sets but does not have the areal coverage (Cotton et al., 1994). In particular the MAPS data set only extends approximately 180 kilometers east of West Palm Beach, Florida. The southern extent of the MAPS data set does not include the Yucatan Peninsula or much of the southwest Gulf of Mexico. Large portions of the model domain used in these simulations are outside the MAPS domain. Therefore the model was initialized using the NMC data archived at NCAR. The ISAN package was partially performed

on the Cray YMP at NCAR and the files transported back to CSU for local use. Isentropic analyses were performed valid at July 29/12Z and July 30/00Z, the beginning and end of the study period. A description of the ISAN package can be found in Tremback (1990), Cram (1990) and Pielke et al. (1992).

The ISAN package first assimilates data from the NMC global analysis combining horizontal winds, temperature and relative humidity as a function of pressure. The second step is the isentropic stage which combines the pressure data from stage one with surface observations and rawinsonde data and interpolates these data sets to a series of isentropic surfaces. A Barnes objective analysis is performed to smooth fields before the final stage is performed. The first two stages were performed at NCAR and the third stage of the isentropic analysis was performed at CSU on a Stardent 3040. The last step in the ISAN package is to interpolate the isentropic data to the model surfaces. After the isentropic analysis files are created the actual model may be implemented.

2.2 The Model Package

The model package uses the isentropic analysis performed by ISAN and with the chosen physics and dynamics of the model makes a forecast of how the atmosphere will appear in the future. There is a long list of physical and dynamical options available for use with the RAMS model. Pielke et al. (1992) has a comprehensive list of the various options. RAMS predicts u , v , and w components of the wind, dry air density, ice/liquid potential temperature Θ_{il} , total water mixing ratio and the mixing ratio for the water species (rain, snow, pristine ice, aggregates and graupel). Using these variables pressure, potential temperature, cloud mixing ratio and vapor mixing ratio are calculated. Many variables are derived from these using the VAN package to display the model results.

2.2.1 Model Numerical Procedures

The model uses non-hydrostatic and compressible forms of the primitive equations (Tripoli and Cotton, 1980) on an Arakawa type C grid. Scaler variables are defined at the center of each grid and the velocity is defined at the grid face. Vertical and horizontal advection was performed using a second order leapfrog advection scheme and centered

spatial derivatives (Tripoli and Cotton, 1982). The advection scheme uses an Asselin filter and a time-splitting routine to integrate the acoustic terms on a short time step.

The largest grid had a time step of 90 seconds while the smaller grids had long time steps of 45 and 22.5 seconds each. A time-splitting routine is used that allows the prognostic variables in the pressure gradient force and divergence equations to be calculated on a smaller time step. A ratio of 1:3 was specified for the simulations for the time splitting routine. Additionally, the speed of sound can be artificially lowered to achieve greater computational efficiency for the acoustic subroutine with little alteration in the quality of the solution (Droegemeier et al., 1987).

2.2.2 Boundary Conditions

Boundary conditions represent one of the areas where regional mesoscale models have problems. Anthes (1983) noted that lateral boundary conditions are a major source of errors in regional models. Because of the limited domain of the model methods must be established to allow information to cross the boundary. Usually this involves allowing internally generated waves to pass out of the domain and allowing meteorologically significant information to propagate into the domain (Anthes, 1983). The boundary conditions were specified by using the Davies nudging scheme on the outer five grid points of the large grid. At each time step the model calculates an observed field from the fields derived in the isentropic analysis. It then compares the modeled field to the "observed" field and nudges the model toward the observed fields. Weighting factors used for each grid point were recommended by the Walko and Tremback (1992) but may be changed by the user.

Boundary conditions at the top of the model domain are specified as a rigid lid. The only other choice for upper boundary conditions in the non-hydrostatic configuration is to use the Klemp/Durran (1983) scheme. Both of these schemes have their drawbacks. The wall on top tends to reflect gravity waves back into the domain (Heckman, 1991) and the Klemp/Durran boundary conditions do not work well in the presence of strong convection. To avoid gravity waves propagating back into the domain a Raleigh friction layer was added to the top five model layers. The version of Rayleigh friction used in this simulation differs from that used by Cram (1990) and Heckman (1991) in some important

ways though. The standard Rayleigh friction scheme used in RAMS uses a Newtonian relaxation scheme from the model state to some reference state. In the standard code this reference state is taken from the horizontally homogeneous initial conditions. Cram used a spatially averaged reference state to relax toward. This scheme is computationally expensive in a horizontally variable initialization, as in these simulations. A more efficient time varying Rayleigh friction scheme was developed by Walko (personnel communication) for use with the 2.5w cumulus parameterization scheme in the original 2c code. This code was modified slightly to be compatible with changes in the new 2c code. This version averages toward a time varying state dependent on the isentropic analysis. The module that initializes the model was changed slightly from the original 2c code to the new 2c code. These changes were incorporated into the code developed by R. Walko to make it compatible with the new code.

2.2.3 Eddy Diffusion

The eddy diffusion coefficients are defined at the thermodynamic point of an Arakawa type-C grid. The horizontal diffusion coefficients are calculated using a deformation rate equation first proposed by Smagorinsky. The horizontal diffusion coefficients are modified by the Richardson number depending on the stability of the atmosphere. For a more detailed discussion see Lilly (1962). Vertical diffusion is handled by the 2.5w cumulus parameterization.

2.2.4 Cumulus Parameterization

The standard RAMS configuration uses a Kuo-type parameterization scheme. This scheme is very simple and computationally efficient. The Kuo scheme was first developed in 1965 and remains one of the most popular schemes. The scheme has been improved on numerous times including Kuo (1974), Kanamitsu (1975), and Krishnamurti et al. (1976), Anthes (1977), and Bougeault (1985). The Kuo scheme used in RAMS is based on work by Tremback (1990). The Kuo-type schemes is driven by the low level moisture convergence. A one dimensional cloud model is used to redistribute the heat and moisture in the vertical. Kuo (1974) introduced a partitioning function to distribute the low level moisture

convergence between heating and moistening the upper atmosphere. When moisture enters the cloud base it has a certain amount of energy that it is capable of releasing due to its latent heat. The question that concerns modelers is how that moisture is partitioned in the upper atmosphere: how much remains moisture and how much energy is released. This partitioning function determines how the temperature and moisture profiles evolve, both spatially and temporally. Schemes exist to calculate it based on relative humidity or the large scale vertical velocity and vorticity (Bougeault, 1985). The cumulus parameterization scheme used by MM4 specifies the partition function as a function of height (Warner and Seaman, 1990).

Bougeault also introduced the concept of a cloud mass flux (1985) in adjusting the Kuo scheme. The solution of the partitioning parameter is one the largest drawbacks to the Kuo type schemes. Depending on how the solution is defined the future state of the atmosphere changes. Tremback's (1990) version calculates the partition function based on an empirical formula.

There is at least one parameterization that solves the partitioning function explicitly. In addition to avoiding the problems associated with approximating the partitioning function the scheme is not limited to large grid sizes; the scheme is designed for grids in the 5-50 kilometer range (Weissbluth and Cotton, 1994). Most cumulus parameterization schemes are restricted to larger grid sizes. This is because the subsidence is assumed to occur in the same grid volume that the convection occurs in.

This scheme is based on a 2.5 order turbulence scheme in which the equations are closed by the variance of the vertical velocity, hence the name 2.5w. This differs from a standard 2.5 level model that closes on the turbulent kinetic energy, TKE. The decision to close the equations on the vertical velocity variance, $\overline{w'w'}$, was made for a number of reasons. First, $\overline{w'w'}$ allows for vertical and horizontal advection to be done explicitly. This is vastly different than the Kuo scheme and most other cumulus schemes that require the convection and its effect on the environment to be enclosed in a single grid volume. By allowing $\overline{w'w'}$ to be advected explicitly adjacent grid volumes can communicate directly. Second, the vertical velocity variance can respond to shear since it is advected. Because of this the shear production term in the vertical velocity variance time tendency equation

may be solved. Additionally, Weissbluth (1991) noted that the vertical profile of $\overline{w'w'}$ was very similar for tropical squall lines and a mid-latitude supercell. This would imply that the vertical velocity variance behaves the same independently of its environment. Furthermore, $\overline{w'w'}$ profiles have the same general shape as the vertical fluxes of total water, microphysical variables, and ice-liquid potential temperature, Θ_{ii} .

In addition to simulating small-scale convective scale turbulence a convective adjustment scheme is used when the criteria for deep convection is met in the 2.5w scheme. This is done by using a cumulus flux scheme similar to Betts (1975). The turbulence parameterization terms have been included to account for the effect of water loading on the buoyancy terms. This also allows the 2.5w cumulus scheme to act as a source function for the host models hydrometers. In the case under study this allows the one dimensional cloud model to communicate with the rest of the RAMS model. The convective adjustment term allows the updraft to be warmed and moistened. Weissbluth (1991) determined that the mass flux rate for mid-latitude storms quadrupled while tropical storm mass flux rates only doubled. The mass flux rate is one of the variables included in the parameterization and is user specified.

The downdrafts are assumed to be driven by precipitation and evaporation. The evaporative pressure scale is used to estimate the evaporation in the downdraft and therefore determines the downdraft characteristics. This is also one of the variables used in the parameterization and is user specified. Weissbluth (1991) found values of 240 mb for the mid-latitude supercell and 180 mb for the tropical squall line as representative values.

In addition to parameterizing both updrafts and downdraft separately in the 2.5w scheme the deep convection cloud fractional coverage is also calculated. This parameter is dependent on both the grid size and environmental conditions. The deep convective cloud fractional area is based on knowledge of draft fractional area, the environment and the grid size (Weissbluth, 1991). The draft fractional area is based on knowledge of the grid size and the bulk Richardson number, which allows the calculation of the deep convective cloud fractional coverage.

The 2.5w scheme has several advantages over other cumulus schemes. Other convective schemes are triggered when the grid scale vertical velocity exceeds some threshold value. In

addition to starting convection in this manner the 2.5w scheme also allows convection to be initiated if the vertical velocity variance exceeds some value. Both of these parameters are grid and environment dependent. Larger grids require smaller values to trigger convection. Additionally, tropical environments generally have lower threshold values. This feature allows a squall line to self-propagate since the $\overline{w'w'}$ produced by the downdrafts continues to excite new convection. The threshold values for w and $\overline{w'w'}$ are user specified.

2.2.5 Microphysical Parameterization

As described by Flatau et al. (1989) RAMS can simulate moisture in any one of four ways:

- 1) completely dry, ignore water vapor
- 2) moisture as a passive tracer, allows supersaturation to occur with no consequences
- 3) supersaturation condensation, any supersaturation is condensed out of the atmosphere as liquid water
- 4) full bulk microphysics, individual ice and water species are predicted or specified by the user.

The bulk microphysics is used to take full advantage of the 2.5w parameterization code. The cumulus parameterization scheme includes hydrometer profiles which can be transmitted back to the host model. Because the hydrometers can be used by the host model it is consistent to use the microphysical module of RAMS. The mean diameters of rain, aggregates, and graupel are specified in the model as 0.054 cm, 0.33 cm, and 0.1 cm, respectively. Pristine ice crystals are a prognostic variable of the model and snow is not allowed. The microphysical parameters are specified for each grid. The same parameters are used on all three grids, but is not necessary. Additionally, aerosol parameters were consistent with a maritime tropical air mass.

2.2.6 Radiation Parameterization

The long and short wave radiation scheme described by Chen and Cotton (1983, 1987) is used in this simulation. This scheme incorporates radiation effects due to molecular

scattering, ozone absorption, absorption by clouds, emission by clouds, and emissivity of clear air and cloudy layers. There is another radiation option in RAMS developed by Mahrer and Pielke (1977) that is more computationally efficient. It gains this efficiency in part through neglect of the effect of cloud reflection and absorption of short wave radiation. Because of this surface temperatures and cloud formation are adversely effected by using the Mahrer/Pielke scheme.

2.2.7 Surface Parameters

The topography is defined on the large grid using a 10 minute data set and a 30 second data set on the smaller grids. The 10 minute data set is used because the topography is not defined in Mexico or Cuba in the 30 second data set. Print statements warning of missing topography files over the ocean were commented out of the model code. The soil model developed by Tremback and Kessler (1985) is used to parameterize the soil temperature and moisture. An initial soil temperature gradient is specified in the model consistent with an early morning profile. The soil model consisted of eleven levels from the surface to 1.3 meters below the surface. The model was initialized with a horizontally homogeneous vegetation cover of short grass, one of 18 possibilities for use in RAMS. The model also used a surface layer parameterization scheme described by Louis (1979). Additionally, the sea surface temperatures were initialized using climatological data from NCAR.

2.2.8 Changes from the standard code

For the simulations performed for this study the standard new 2c model code was used with the following exceptions.

- 1) rcnfg2c- which contains storage space for the model parameters, changed by Weissbluth to handle extra parameters in the 2.5w scheme.
- 2) rconv2c - contains the 2.5w convective parameterization version rconv2c.anu developed by Weissbluth. Changed by the author to plot draft and micro-scale drafts at each analysis time instead of every time step.
- 3) rclld2c - contains the cloud model used by the convective parameterization, version rclld2c.anu developed by Weissbluth for the 2.5w scheme .

- 4) `rdriv2c` - model driver altered by Weissbluth for use with the 2.5w scheme, further modified by the author so that the soil temperatures and moistures were not overwritten on restarting the model. The code was also modified so that the sea surface temperatures, percentage of land, and topography were not printed to save file space.
- 5) `rsurf2c` - soil and vegetation parameterizations, the convective precipitation is not counted in the surface fluxes but is added into the host model as liquid water. This change is due to the 2.5w convection parameterization and was changed by Weissbluth.
- 6) `rname2c` - changed from the standard code to allow it to read the extra parameters required by the 2.5w scheme, altered by Weissbluth.
- 7) `rprnt2c` - controls the printing of variables, this module was changed by Weissbluth to allow the plotting of the parameterization variables.
- 8) `rvarr2c` - changed the Raleigh friction scheme derived by Walko for the original version of 2c using the 2.5w parameterization to be compatible with the new 2c code, changed by the author.
- 9) `rinit2c` - contains code to initialize the model, commented out statement to print if a topography file is missing. Due to the large amount of ocean in the domain the model was generating several hundred of these messages. Changed by the author.

2.3 The VAN Package

The VAN package is used to post-process the model output. A variety of parameters may be plotted using a NCAR Graphics routine. The modules of the VAN package used for my simulations were developed by Greg Thompson. These modules offer several advantages over the standard 2c code. Thompson's code plots several parameters in addition to the standard parameters plotted by RAMS. Temperature may be plotted in Celsius or Fahrenheit in addition to the standard plots in Kelvin. Dewpoints may also be plotted, unlike the standard code. The biggest change though is the ability to plot a skew-T chart at any grid point in the domain. This feature is extremely advantageous to observe how the atmosphere changes with time at a location.

2.4 The Domain

The domain of the simulation is plotted in polar stereographic coordinates centered at 29 N and 83 W. The domain extends from Washington D.C. south to the western edge of Hispaniola; it continues to the west to Fort Worth, Texas and north to Topeka, Kansas. This domain is covered by a grid having a 80 kilometer grid spacing. The grid size was chosen such that any synoptic-scale phenomena moving into the grid would normally take at least 48 hours to reach central Florida. The grid also extended well east of the Atlantic coast to detect any tropical easterlies approaching the coast; see Figure 2.1.

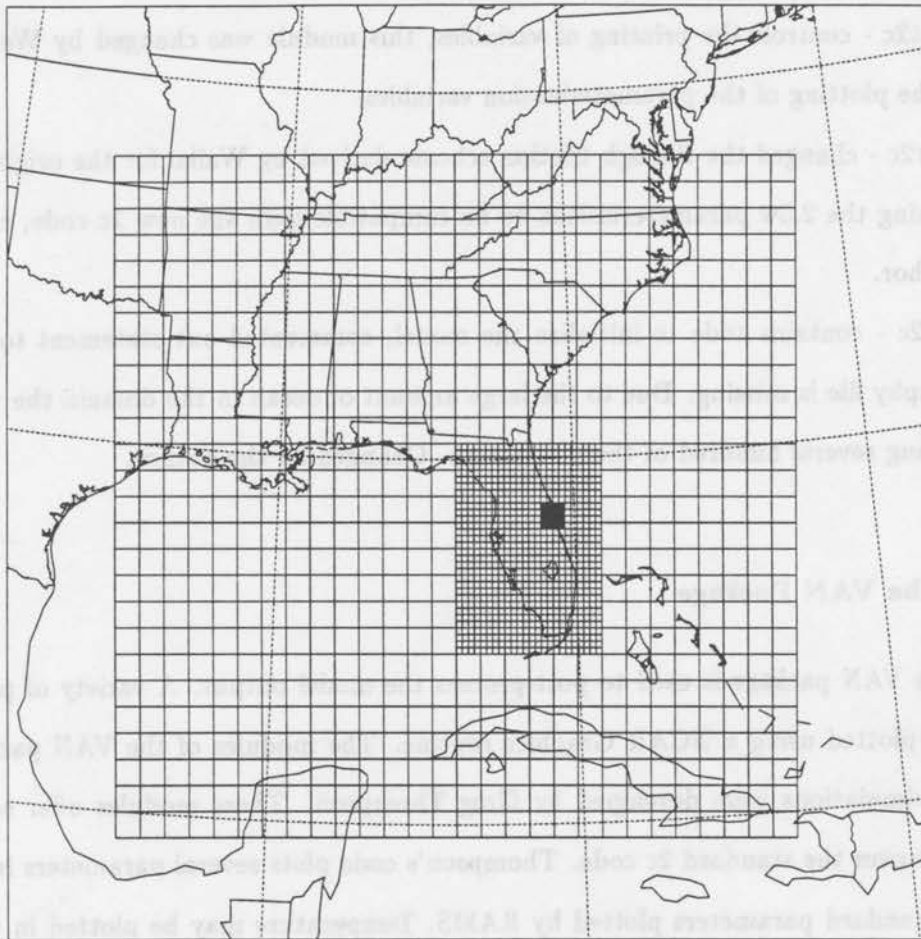


Figure 2.1: Model Domain. Grids 1, 2, and 3

A second grid with a 20 kilometer spacing covers most of the Florida peninsula. The northern boundary is the Okefenokee swamp near the Florida/Georgia border and extends south to the Florida Keys. The western edge is approximately Tallahassee in the panhandle

region and the grid extends 80 kilometers offshore at West Palm Beach. This covers the peninsula and adjacent waters with sufficient detail to provide regional forecasting capability.

The third grid is centered around the Kennedy Space Center, KSC. The grid extends 40 kilometers north-west-south of KSC and 20 kilometers over the ocean to the east. See Figure 2.2 for a detailed view of the third grid. This last grid will be used to evaluate the usefulness of producing TAF's with a mesoscale model and was chosen in part because of the data available from the CaPE experiment to verify the model simulation.



Figure 2.2: Grid 3 domain. Centered over the Kennedy Space Center

The vertical grid began with a vertical grid spacing of 100 meters. This was stretched by a ratio of 1.12 to a maximum spacing of 1000 meters. The first model level was 48 meters above the surface. This spacing allows a high resolution in the lowest levels of the atmosphere which is critical to aviation forecasting. There are eight levels below 900 meters, 3000 feet, which significantly enhances the models ability to detect clouds in the area of concern to the aviation community. The domain extended to a height of 21.7

kilometers, almost 69000 feet. While this may seem high the Raleigh friction layer begins at 17.7 kilometers or approximately 58000 feet. Radar summaries for the day indicate no thunderstorms above 16.5 kilometers (54000 feet).

The third grid is centered around the Kennedy Space Center, KSC. The grid extends 40 kilometers north-south of KSC and 20 kilometers over the ocean to the east. See Figure 3.3 for a detailed view of the third grid. This last grid will be used to evaluate the usefulness of producing TAF's with a mesoscale model and was chosen in part because of the data available from the CAPS experiment to verify the model simulation.



Figure 3.3: Grid 3 domain. Centered over the Kennedy Space Center.

The vertical grid began with a vertical grid spacing of 100 meters. This was stretched by a ratio of 1.12 to a maximum spacing of 1100 meters. The first model level was 45 meters above the surface. This spacing allows a high resolution in the lowest levels of the atmosphere which is critical to aviation forecasting. There are eight levels below 600 meters, 3000 feet, which significantly enhances the models ability to detect clouds in the area of concern to the aviation community. The domain extended to a height of 21.1.

Chapter 3

RESULTS OF THE RAMS SIMULATIONS

3.1 The Experiments

There are a number of variables that can be specified by the user in the RAMS name list. The numerical method options were described in Chapter 2. In the name list the user may specify: diameter of the microphysical species, frequency of the analysis and history files, the number of points in the Davies nudging region and their weights, the number of points in the Raleigh boundary region and the dissipation time scale, the threshold value to activate the convective parameterization scheme, and the vegetation type used in the simulation. Once these were decided upon they were not changed throughout the course of the simulations. The values specified in the model were chosen in accordance with the RAMS User's Guide (Walko and Tremback, 1992) for a sub-tropical environment.

The frequency of analysis was 1 hour. The frequency was chosen for a variety of reasons, chief among them was space. Analysis files are created for each grid at the frequency interval specified. Additionally, a header file is created at each analysis time interval. This creates analysis files of approximately 3.3 megabytes each time the analysis is performed. The model also creates a standard output file approximately 2 megabytes in size. The 2.5w cumulus parameterization scheme also produces a graphics package to allow the user to view the parameterized values and their evolution over time. In these simulations the draft scale parameters were plotted at the expense of another 2 megabytes. This requires computer space of around 40 - 50 megabytes for a 12 hour simulation analyzed every hour.

The model produces history files at any user specified intervals. The files are used if it becomes necessary to start the model at some time after the beginning of the simulation. For instance, if the model is begun at 12Z and a history file is created at 15Z it is possible to start the model at 15Z and not perform the first three hours of the simulation again.

This feature is beneficial in a research environment where it can prevent needless number crunching but I chose to forego this option. The decision was based on two considerations. First, I was performing a 12 hour simulation so the time necessary to start the model from the beginning was not exorbitant. Secondly, each history file is approximately 10 megabytes. The cost in disk space to save a file of questionable use was too great given the computer resources. There are other environments though where this option is of great use.

The vertical velocity threshold value to activate the cumulus parameterization was chosen to be 0.0 m/s. This value is a grid average value and assures that the scheme is not activated in an area of general subsidence. This threshold value is specified in the name list for the host model, RAMS. The other name list variables were discussed in Chapter 2.

In addition the 2.5w cumulus parameterization scheme also has several variables that are specified by the user. Among these are: the threshold values for the vertical velocity and the vertical velocity variance, the entrainment rate, evaporative pressure scale, and the maximum boundary layer height. The vertical velocity term in the 2.5w scheme is a threshold to activate the parameterization and is a different threshold from the name list threshold. The two terms are not required to agree. Also, the name list threshold only initiates the convective scheme whereas the threshold value for the 2.5w scheme is grid dependent. A value for the vertical velocity variance threshold was recommended to be $1.3 \text{ m}^2/\text{s}^2$ and was also not changed in the simulations. Additionally, the condensate partitioning terms for the updraft and downdraft may also be specified (Weissbluth, 1991). To change the partitioning functions the one dimensional cloud model code must be changed. Since the ultimate objective of this research is to provide an operational forecasting model it is not practical to change code routinely so the partition functions were not changed. It also is not practical to change the 2.5w code so that other users will not be prevented from easily adapting this work to other topics.

Numerous experiments were performed by varying the vertical velocity threshold, evaporative pressure scale, entrainment rate, and the maximum boundary layer height.

When the 2.5w scheme was developed the values for the parameters were determined for a mid-latitude supercell and a tropical squall line (Weissbluth, 1991). Using these values as limits intermediate values were tried. A reasonable first guess was that the thunderstorms

in Florida were more tropical in nature than mid-latitude, especially in July. The values determined to be the best were:

vertical velocity = 0.007, 0.05, 0.1 m/s

evaporative pressure scale = 20000 Pa

entrainment rate = 2.5

maximum boundary layer height = 1000 m.

In this chapter we will discuss the results of the best model run and compare the simulation to another simulation using the Mahrer/Pielke radiation scheme.

3.2 Synoptic Conditions

The surface and upper air charts at 12Z 29 July foretold of thunderstorms throughout Florida by the afternoon. The National Meteorological Center (NMC) surface chart valid at 12Z 29 July analyzed a low pressure system along the North Carolina/Virginia border. A stationary front was located through the central Carolinas and meandered through the deep south until it weakened in a high pressure system north of New Orleans. A second frontal system was anchored in Illinois and the associated cold front trailed through northern Texas to near Amarillo; see Figure 3.1.

The surface chart of the model initialization does not clearly indicate the low pressure system in Illinois but there is the hint of the front in the sea level pressure analysis; see Figure 3.2. The stationary front is well depicted though. The cyclone is well defined along the North Carolina/Virginia border. The front is evident throughout the South and terminates in an anti-cyclone in Louisiana, just as the NMC surface depiction. A high pressure ridge extends southwest through northeast from the Lower Keys to the northern Bahamas. There is a second trough that is barely evident along the western coast of Florida. This feature is not analyzed on the NMC surface chart but will act as a trigger for convection later in the day. The 1012 mb high over the Yucatan Peninsula is an anomaly of the initialization of the model.

The model adjusts the pressure field within the first hour of the simulation; see Figure 3.3. After this initial adjustment the high pressure anomaly disappears. Most of the detail is

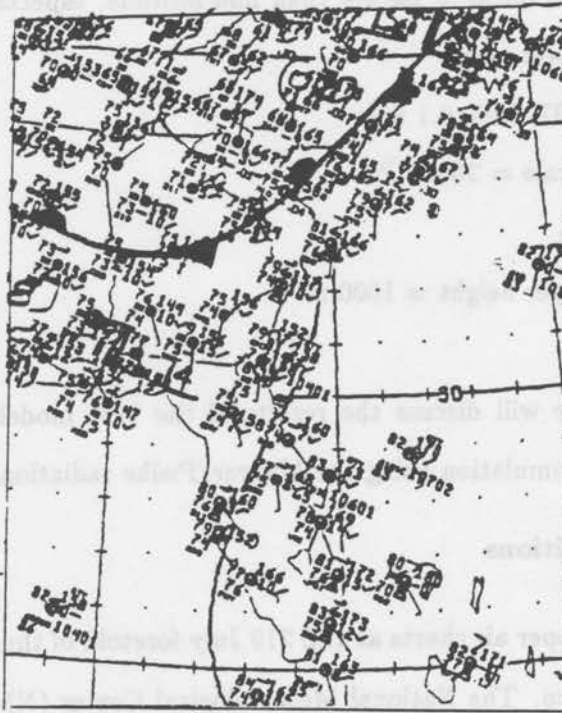


Figure 3.1: NMC analyzed surface chart; 12Z 29 July

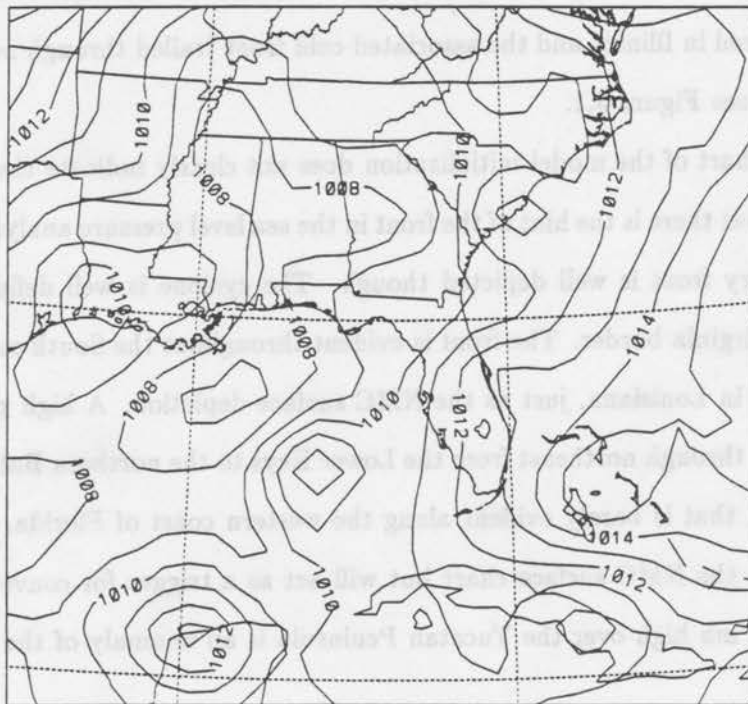


Figure 3.2: Model initialized sea level pressure (mb); 12Z 29 July

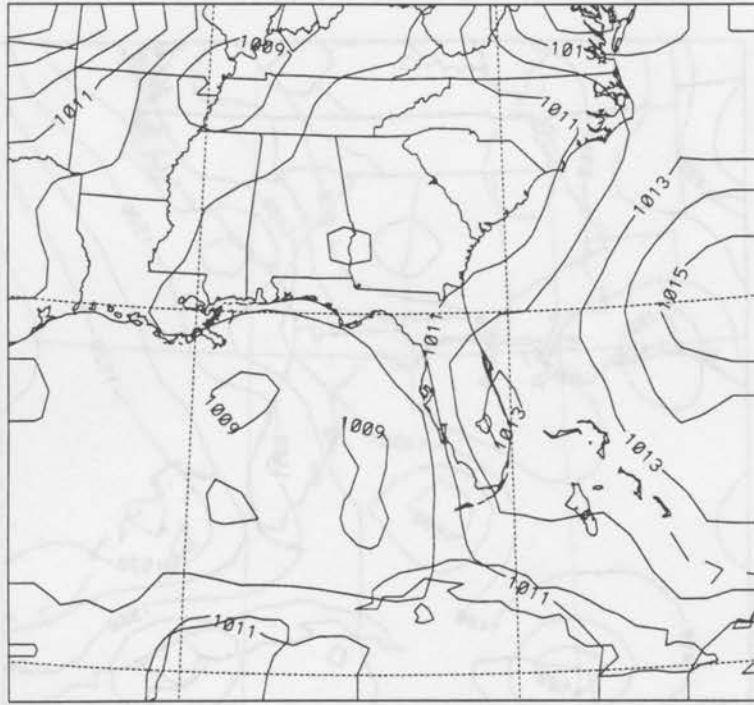


Figure 3.3: Model sea level pressure (mb); 13Z 29 July

also lost from the initial analysis. The stationary front is evident as a large area throughout the central Carolina's extending back to Louisiana. However, the location of the front can not be determined from the pressure analysis. The trough along the western coast of Florida and the ridge through the Keys is analyzed though.

A closed low pressure system at 850 mb over the Georgia/Alabama border is still evident in the model analysis although the front extending from Illinois is not as noticeable; see Figure 3.4. The stationary front is still evident with the gradient aligning with the surface front. The trough is evident along the western coast of Florida. The 850 mb upper air chart indicates that dew point depressions were less than 5 degrees Celsius throughout the entire southeast region; see Figure 3.5.

The trough along the west coast is also observed at 700 mb along with a ridge that is extending from the South Carolina coast inland to the Appalachians; see Figure 3.6.

The ridge is very evident at 500 mb, in both the model initialization and the NMC products; see Figures 3.7 and 3.8. The ridge is more evident in the model than the NMC analysis due to the contour interval. A major short wave associated with the frontal system

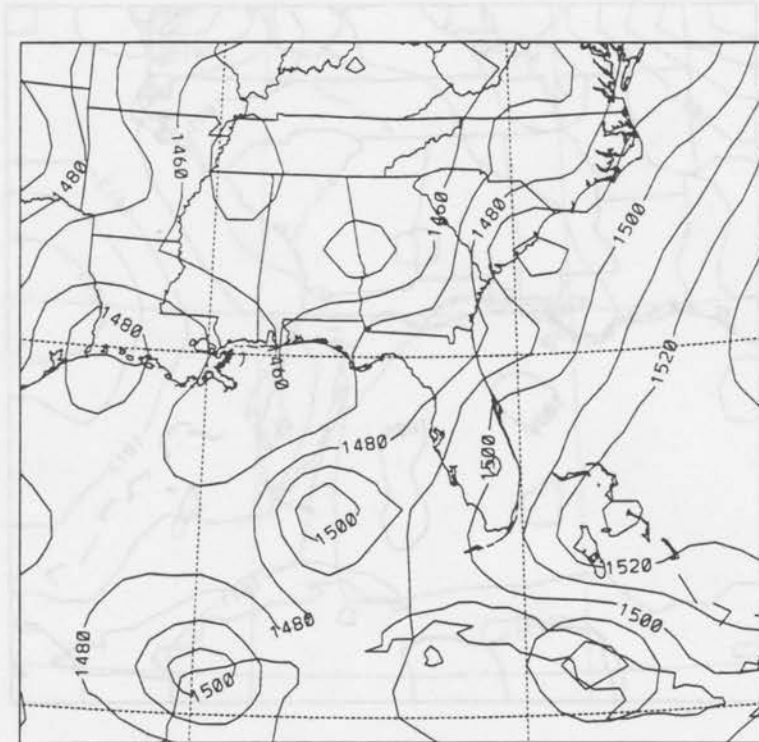


Figure 3.4: Model initialized 850 mb geopotential heights (m); 12Z 29 July

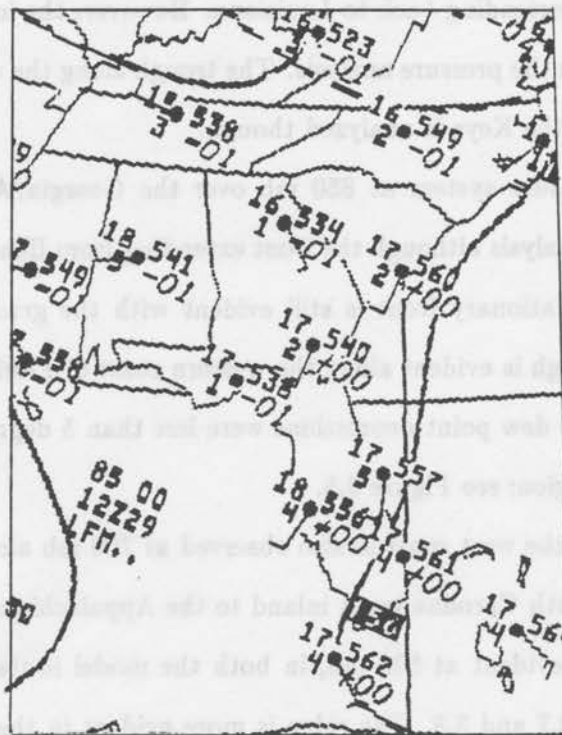


Figure 3.5: NMC analyzed 850 mb upper air analysis; 12Z 29 July

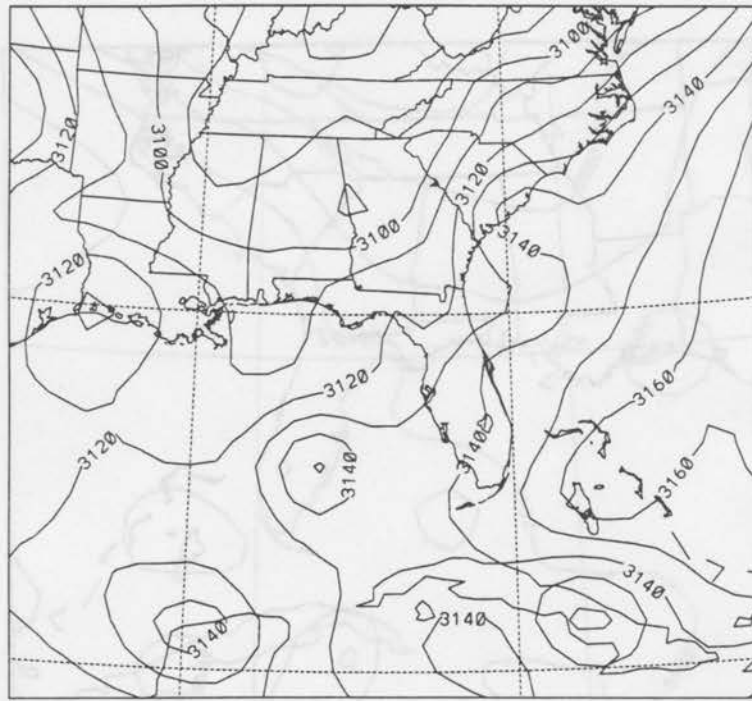


Figure 3.6: Model initialized 700 mb geopotential heights (m); 12Z 29 July

in Illinois is also evident. This ridge is part of the Bermuda High that dominates the weather of the southeastern United States during the summer.

As part of the CaPE experiment rawinsondes were launched at the Kennedy Space Center, KSC. The 1015Z rawinsonde indicated the moisture and stability parameters to be: lifting index=-4, convective temperature= 30.5 °C (87 °F) and precipitable water= approximately 49 mm (1.93 in) (Williams et al., 1992).

The NGM initialization valid at 12Z on 29 July indicated a front through western Illinois back through Arkansas; see Figure 3.9. The stationary front in the southeast is not well depicted on the sea level pressure analysis.

The 700 mb panels indicated relatively humid air with a broad region of air in excess of 70 percent relative humidity; see Figure 3.10. The 500 mb vorticity chart indicates a vorticity maximum over Tampa; see Figure 3.11. The 500 mb NMC analysis (Figure 3.8) indicates that the wind speeds are less than 5 m/s (10 kt) in Florida so there is negligible vorticity advection.

The 12 hour NGM forecast valid at 30/00Z indicates little change in the position of the stationary front. The front is not clearly depicted and is represented as a series of

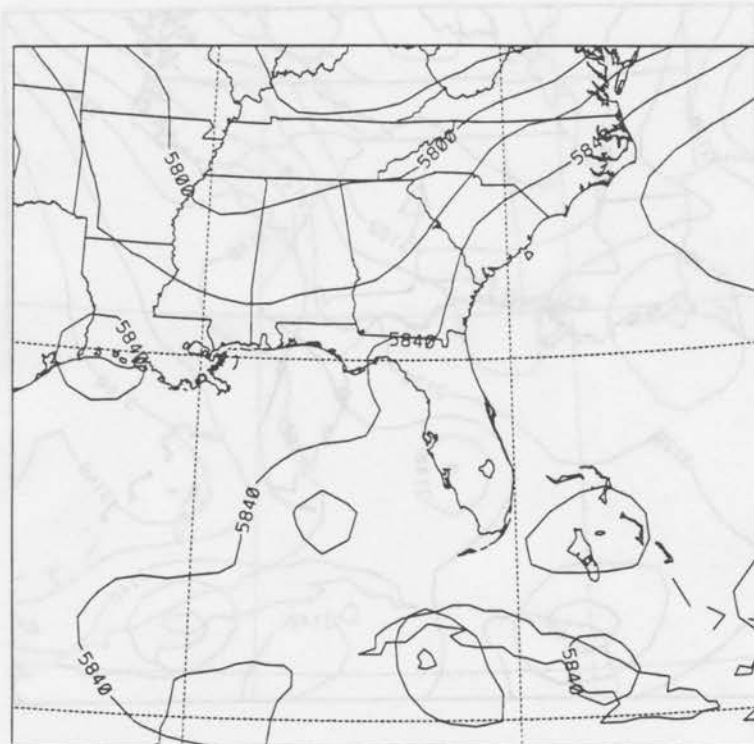


Figure 3.7: Model initialized 500 mb geopotential heights (m); 12Z 29 July

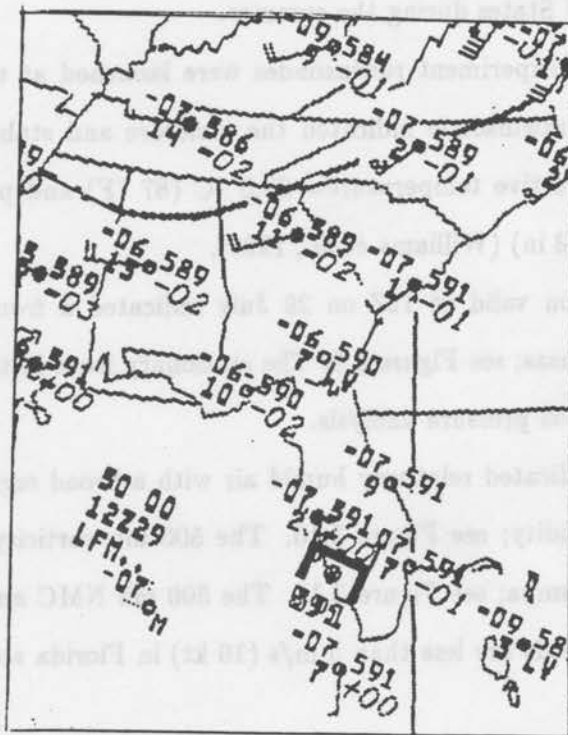


Figure 3.8: NMC analyzed 500 mb upper air analysis; 12Z 29 July

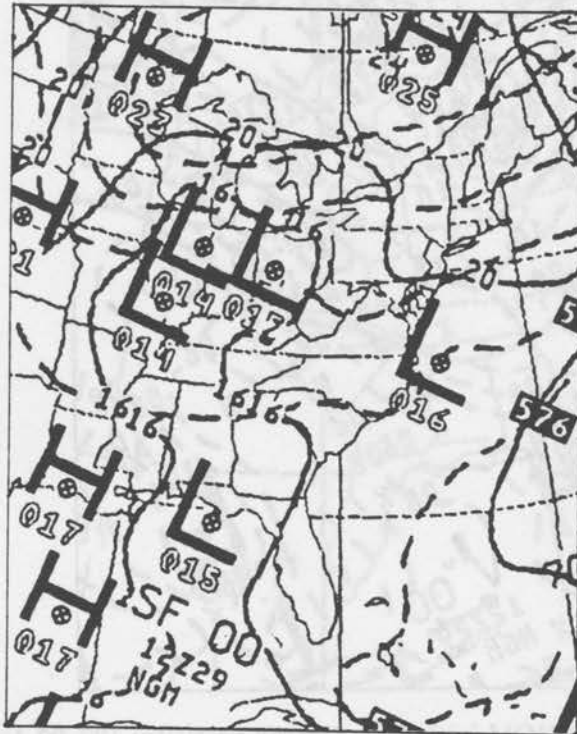


Figure 3.9: NGM initialized mslp (mb) and 1000/500 mb thickness (m) analysis ; 12Z 29 July



Figure 3.10: NGM initialized 700 mb relative humidity; 12Z 29 July

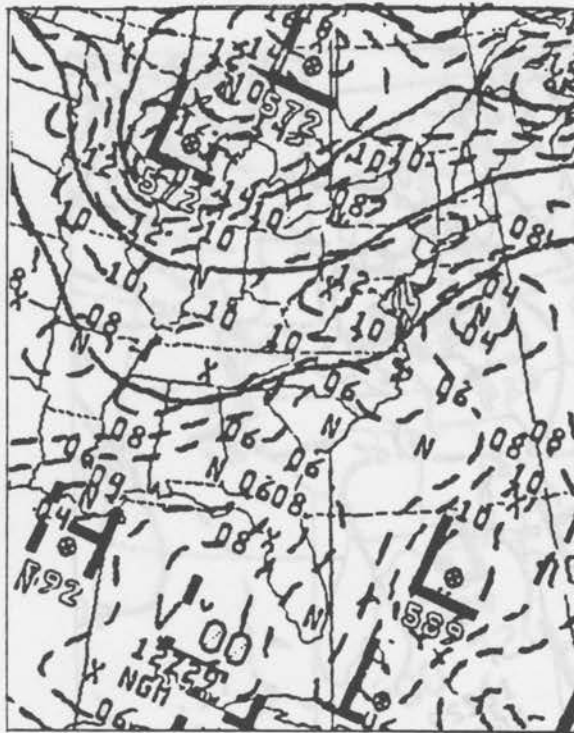


Figure 3.11: NGM initialized 500 mb vorticity; 12Z 29 July

low pressure systems that neither move appreciably or change their intensity; see Figure 3.12. The 700 mb gradient is still weak indicating no strong winds; see 3.13. The 700 mb with relative humidity is still above 70 percent for much of the southeast. Additionally, the vertical velocities are indicated to be $3 \mu\text{b}/\text{sec}$ in central Florida, see Figure 3.14. There is an area of precipitation indicated near Kennedy Space Center of approximately 30 mm (1.18 in). There is also an area of precipitation near Charlotte North Carolina of almost 28 mm (1.09 in).

The 500 mb chart indicates that the vorticity maximum near Tampa has not moved appreciably; see Figure 3.15. This was expected since there was little vorticity advection indicated on the initial NGM analysis.

The stability parameters from the KSC rawinsonde indicated thunderstorms were probable. Given the 700 mb moisture a layer of cumulus clouds is indicated with the chance that some will develop into thunderstorms later in the day. The NGM was predicting the possibility of large rain accumulations in Florida. However, the NGM cannot predict when or where the convection will begin or how it will affect aircraft operations.

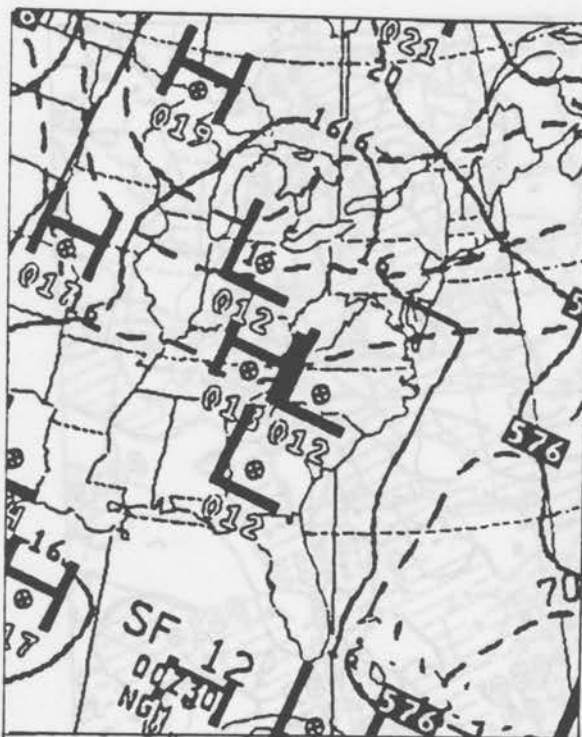


Figure 3.12: NGM 12 hour forecast surface pressure (mb); 00Z 30 July

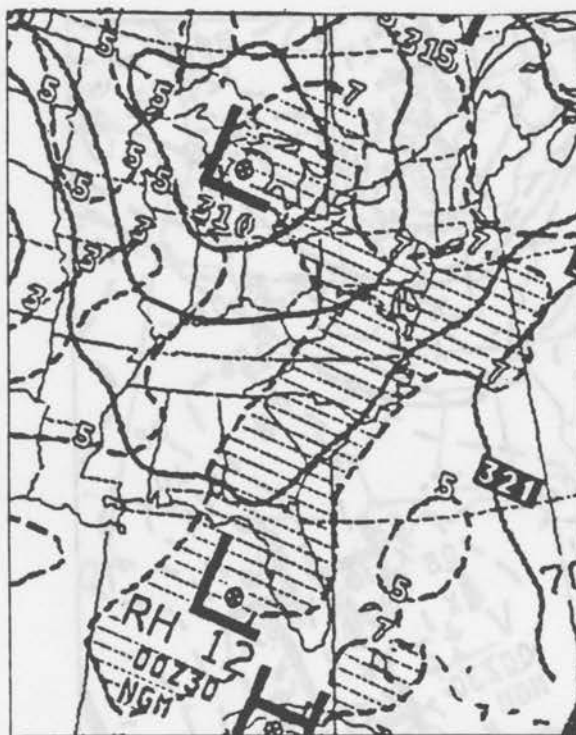


Figure 3.13: NGM 12 hour forecast 700 mb relative humidity; 00Z 30 July

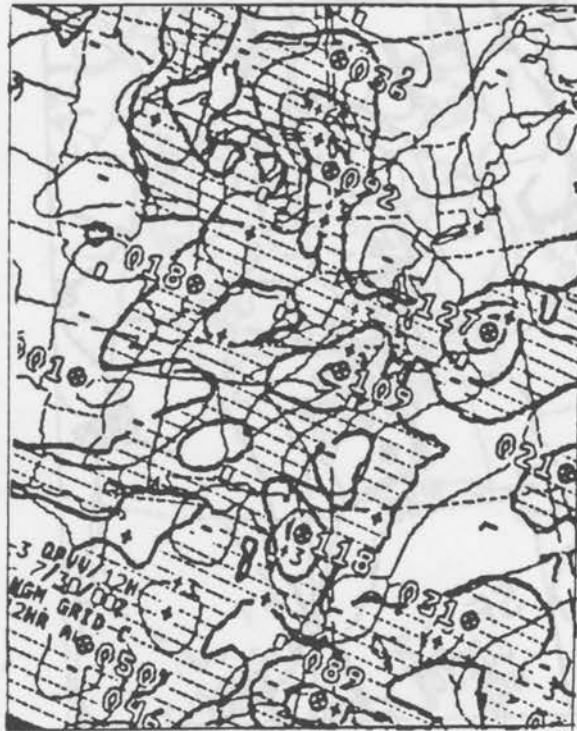


Figure 3.14: NGM 12 hour forecast 700 mb vertical velocities (cm/s) and precipitation (in); 00Z 30 July

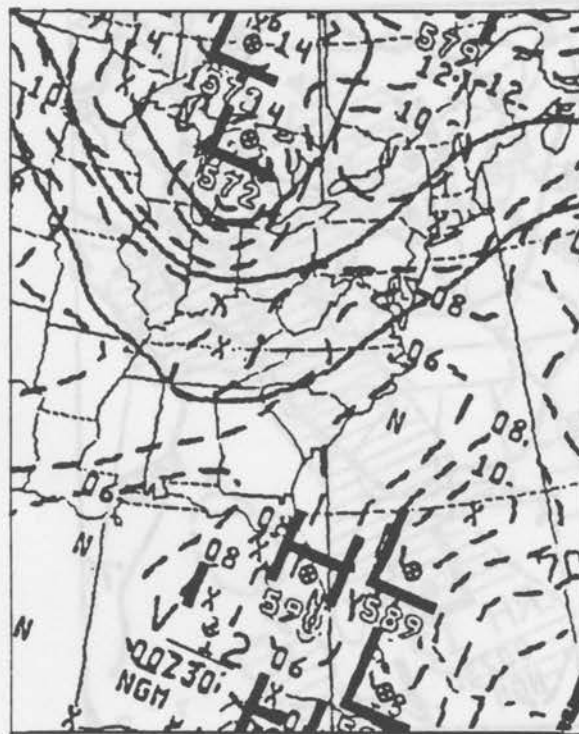


Figure 3.15: NGM 12 hour forecast 500 mb vorticity; 00Z 30 July

3.3 The Control Case

The control case used the parameters stated above and the Chen/Cotton radiation scheme. We will examine the model at several different times. Analyses were performed at 18Z and 21Z on 29 July and 00Z on 30 July. These times were chosen as a matter of convenience. Surface maps and observations were available at these times. The 18Z analysis offers a mid-point in the simulation. The 21Z analysis was chosen after examining the national radar summary. The 2135Z NMC radar summary shows thunderstorm activity throughout the southeast, especially over the Florida peninsula.

The model levels in RAMS are configured so that the first model level is actually below the surface. The second model level is the first model level in the atmosphere. This level is 48.6 m, 160 feet, above ground level and will be considered as near the surface for these simulations.

The 29 July 18Z Analysis

The first field to be examined is the sea level pressure; see Figure 3.16. A trough from central Georgia is still evident extending southeast into the Gulf of Mexico. The trough extending from the Bahamas through the Florida Keys is also depicted well. The NMC surface map ignores the trough in the eastern Gulf; see Figure 3.17. This could be due to the models' ability to isopleth at a much smaller interval than NMC. The standard NMC interval is 4 mb whereas this pressure analysis is every millibar. The NMC surface map indicates no pressure contours south of Richmond Virginia.

The sea level pressure on the second grid is depicted in Figure 3.18. A slight trough is evident along the western coast of Florida. This analysis is consistent with the grid 1 analysis depicted in Figure 3.16.

The temperatures for the second and third grids are depicted in Figure 3.19 and Figure 3.20. The surface temperature from the standard airways observations at 1800Z for Florida are: Jacksonville, JAX, 33; West Palm Beach, PBI, 32; Miami, MIA, 30; Key West, EYW, 33; and McDill AFB, MCF, 27°C. The reported surface temperatures are several degrees

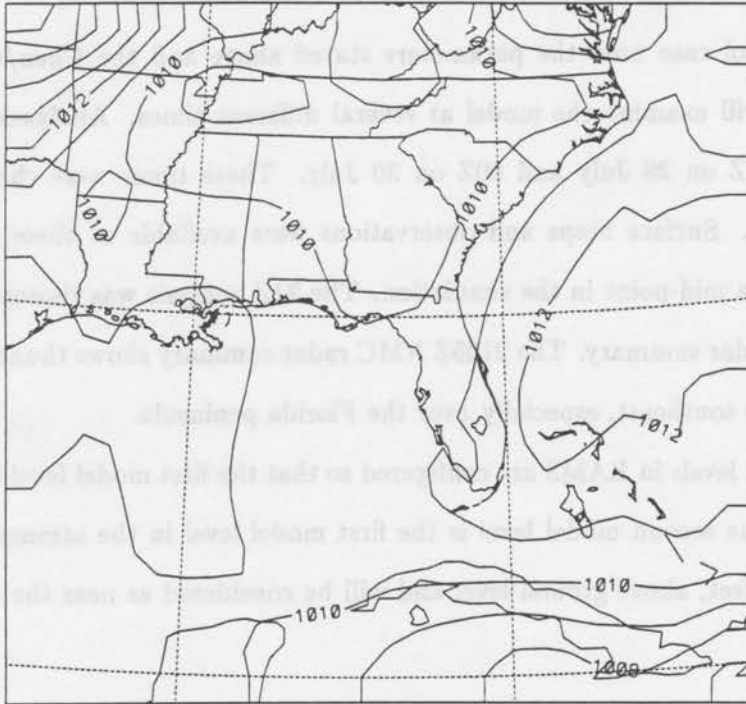


Figure 3.16: Sea level pressure (mb); 18Z 29 July

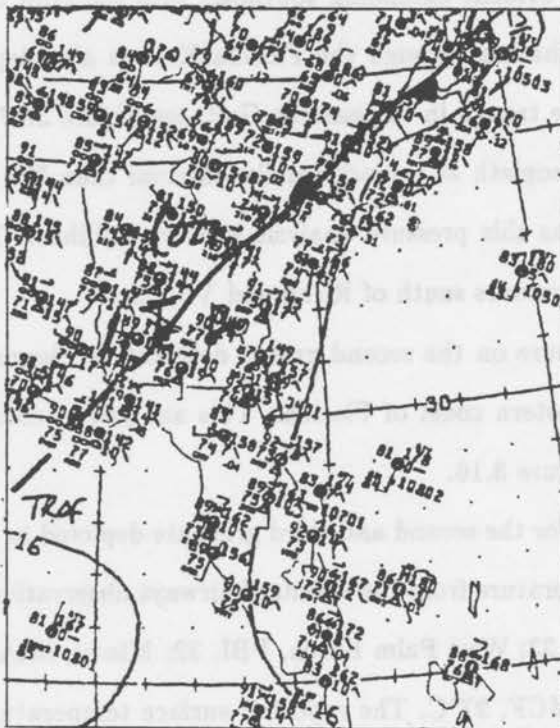


Figure 3.17: NMC surface chart; 18Z 29 July

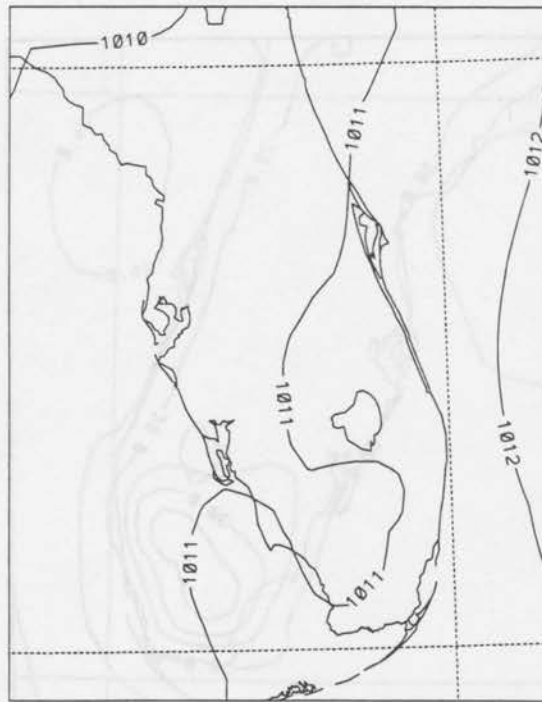


Figure 3.18: Sea level pressure (mb); 18Z 29 July

warmer than the model temperatures. The temperature from the Florida Agriculture network at Tavares reports a temperature of 32°C . Tavares is located approximately in the center of Florida and 10 kilometers north of a line extending east-west through KSC.

Assuming a dry adiabatic lapse rate, the model temperatures at ground level are 0.5°C warmer than the near surface model level, the first model level above ground. While this is not enough to have total agreement between the model simulation and the observations there are two important comments to make. First, the model level is above ground and therefore should be cooler than the observations. Second, the atmosphere is probably super adiabatic, not adiabatic in the lowest level. This would imply that the simulation is in much better agreement with the observations. The temperatures on Grid 3 (see Figure 3.20) closely follow the sea-breeze. Cooler air from the ocean is advected over the warmer land thereby causing a temperature gradient parallel to the coast.

The wind direction and speed near the surface are depicted in Figure 3.21 and Figure 3.22. The winds are in good agreement with observations except in southeast Florida. The winds in MIA are reported as 160° and 7m/s ; winds at PBI are similar. The model winds

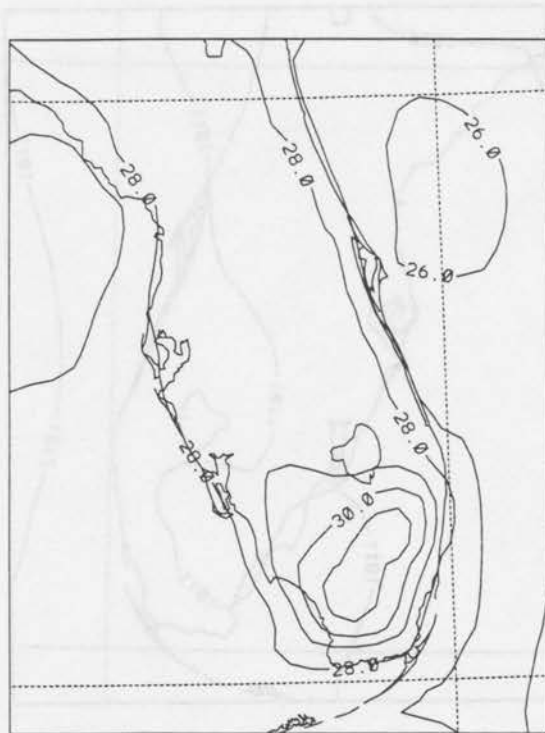


Figure 3.19: Temperature (°C); 18Z 29 July

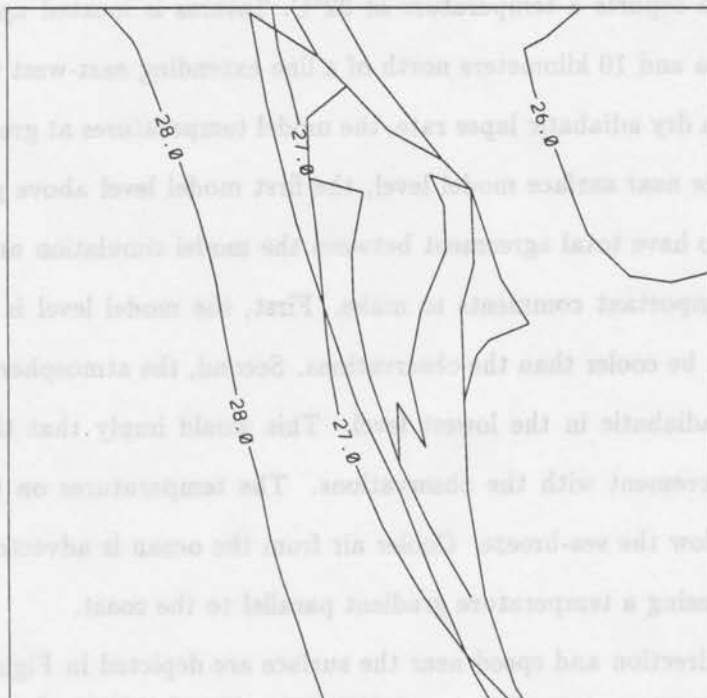


Figure 3.20: Temperature (°C); 18Z 29 July

are approximately 120° and 5 m/s . Winds at Tampa, TPA are 190° instead of the modeled 170° . Winds at JAX are also within 20° . Given the low speeds of the winds this is modeled very well. A convergence zone is detectable from south of Lake Okeechobee through TPA and northward along the west coast. This is consistent with the pressure pattern presented in Figure 3.18.

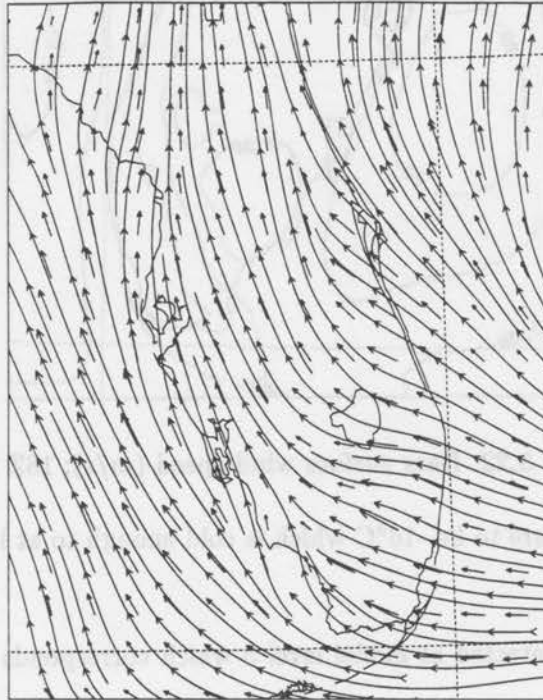


Figure 3.21: Near surface streamlined wind direction; 18Z 29 July

The presence of clouds is not explicitly modeled in the version of RAMS used in this thesis. What is modeled is the explicit calculation of the various microphysical parameters by the microphysical package. Horizontal cross-sections were analyzed at various heights to detect clouds. Model levels 2, 8, and 22 were chosen to detect clouds. These correspond to altitudes of 48.6 m (160 feet), 907 m (2977 feet), and 7679 m (25193 feet). These values were based on criteria for aviation forecast and to determine if the activity was convective. The lowest level is nearly the lowest landing criteria for aircraft. The value of 907 m was chosen because it is approximately 3000 feet which is the threshold for Visual Flight Rules (VFR) for aircraft. The highest level was chosen to determine the extent of any convective activity. A sounding was obtained as part of the Cape experiment at 1015Z from KSC and

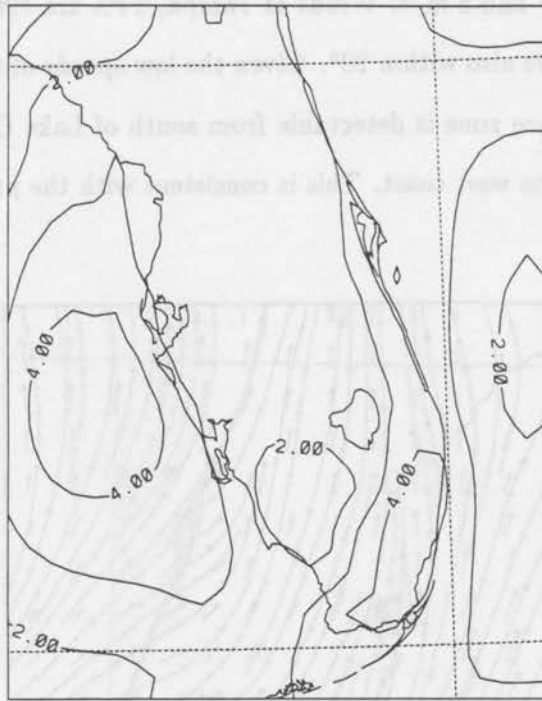


Figure 3.22: Near surface wind speed (m/s); 18Z 29 July

indicated the temperature to be -16°C which is cold enough to at least begin to initiate ice particles.

Cloud water was detected at model level 5 which corresponds to an altitude of 406 m (1330 feet); see Fig 3.23. Cloud water at other levels on the third grid was not detected. The grid spacing implies that the cloud is less than 280 m (870 feet) in depth, the distance between the fourth and sixth model levels.

At 18Z the only other clouds indicated on either the second or third grids were offshore from MIA at an elevation of 7679 m; see Figure 3.24. The mixing ratio contoured is 1×10^{-5} g/g and the parameter plotted is the condensate mixing ratio. This is the summation of all the condensed microphysical parameters. This parameter was chosen to simplify the analysis. Because of the lack of liquid cloud water in the higher altitudes the cloud condensation mixing ratio is of little assistance in finding anything but the strongest updrafts. By contrast the condensate mixing ratio will not only detect any liquid cloud water but also any frozen precipitation. Since there are no clouds indicated below this level the cloud is probably either convection based higher than 900 m or debris from a thunderstorm in Grid 1.

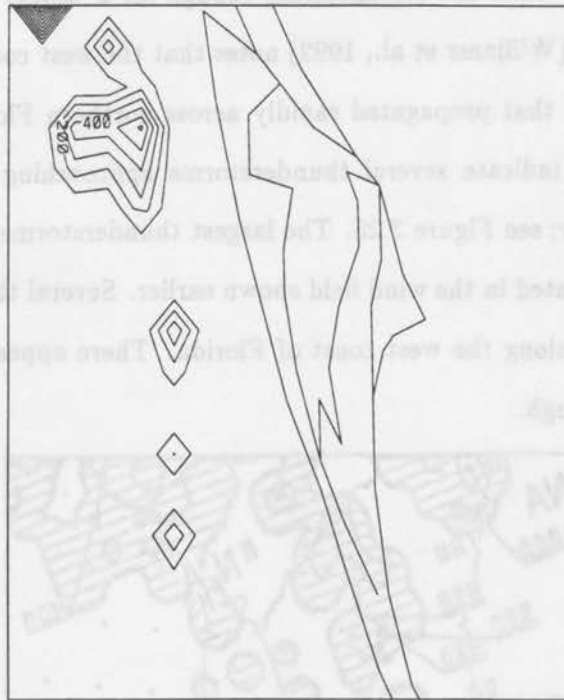


Figure 3.23: Cloud water mixing ratio (g/g), elevation = 406 m, Contour interval = $1 \text{ E-}5$ g/g, maximum contour = $10 \text{ E-}5$ g/g; 18Z 29 July

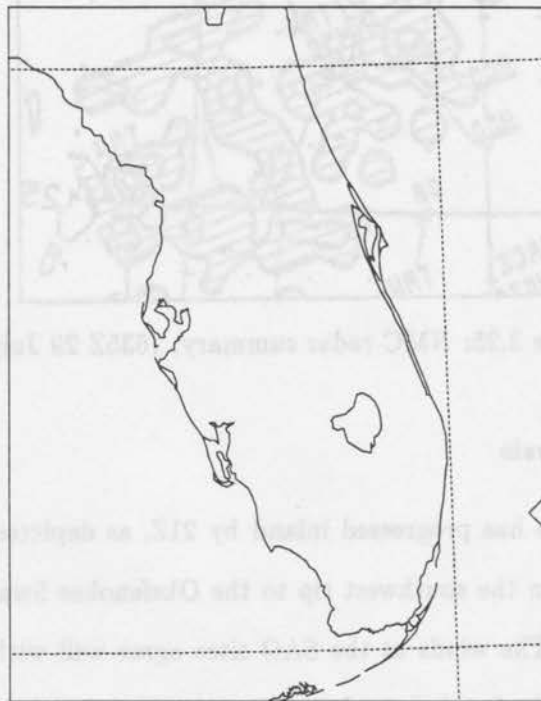


Figure 3.24: Condensation mixing ratio (g/g), elevation = 7679 m contour = $1 \text{ E-}5$ g/g, maximum contour = $1 \text{ E-}5$ g/g; 18Z 29 July

These results are somewhat disconcerting though for a variety of reasons. The CaPE Operations Summary (Williams et al., 1992) notes that the west coast sea breeze triggered thunderstorms by 15Z that propagated rapidly across northern Florida. The NMC radar summaries agree and indicate several thunderstorms approaching 13800 m (45000 feet) on the 1635Z summary; see Figure 3.25. The largest thunderstorms are depicted along the convergence zone indicated in the wind field shown earlier. Several thunderstorms are above 12200 m (40000 feet) along the west coast of Florida. There appears to be no significant activity near KSC though.

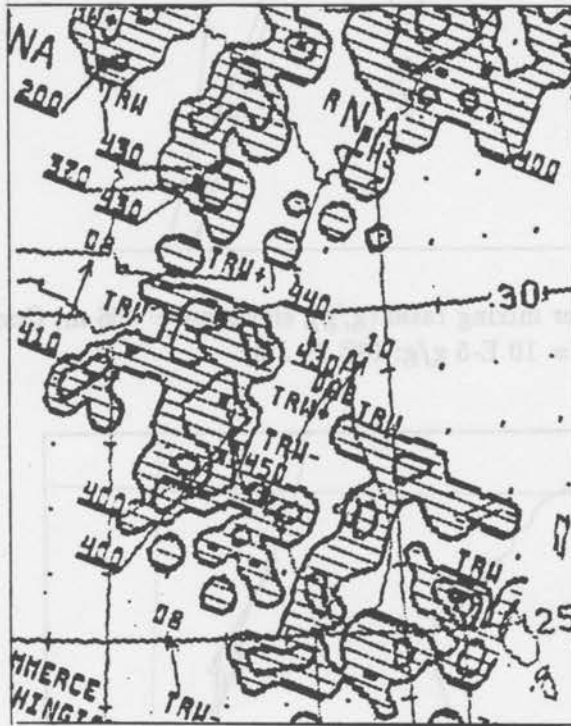


Figure 3.25: NMC radar summary; 1635Z 29 July

The 29 July 21Z Analysis

The convergence zone has progressed inland by 21Z, as depicted in Figure 3.26, and is now from Cape Sable on the southwest tip to the Okefenokee Swamp. The wind speed is shown in Figure 3.27. The winds at the SAO sites agree well with the modeled winds. MIA is still reporting southerly winds and JAX is reporting winds of 210°. Modeled winds at MIA are 130° at 5m/s and JAX is 160° at 6 m/s. TPA agrees very well with observed

winds of 200° at 4 m/s and modeled winds of 200° and 3 m/s. As noted earlier light winds are very difficult to assign a reliable direction to. Winds over KSC are 220° at 5-6 m/s.

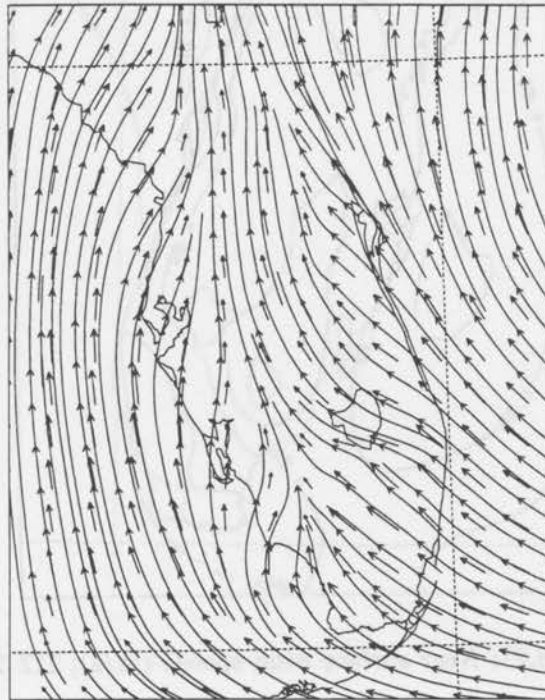


Figure 3.26: Near surface streamlined wind field; 21Z 29 July

Precipitation has occurred since the 18Z analysis; see Figure 3.28 and Figure 3.29. Figure 3.28 indicates heavy showers in southern Florida with more than 12 mm of precipitation falling in 3 hours. There was no precipitation detected on the 18Z analysis. Another area of precipitation is indicated west of KSC. Figure 3.29 indicates that there are two different regions of precipitation west of KSC with more than 12 mm of rain as opposed to 6mm indicated on the second grid; see Figure 3.28. This is indicative of the the problem of resolution. For precipitation to occur on the second grid an area of 400 square kilometers is effected. The third grid only requires initiation of the convective scheme over 25 square kilometers. This concern of when the parameterization is initialized is especially prevalent in analyzing precipitation and the microphysical parameters. The smaller grids are initial-izing convection on a smaller area and the threshold values for vertical velocity are also smaller. The combination of smaller areas and lower vertical velocity thresholds allow the parameterization scheme to be initialized earlier.

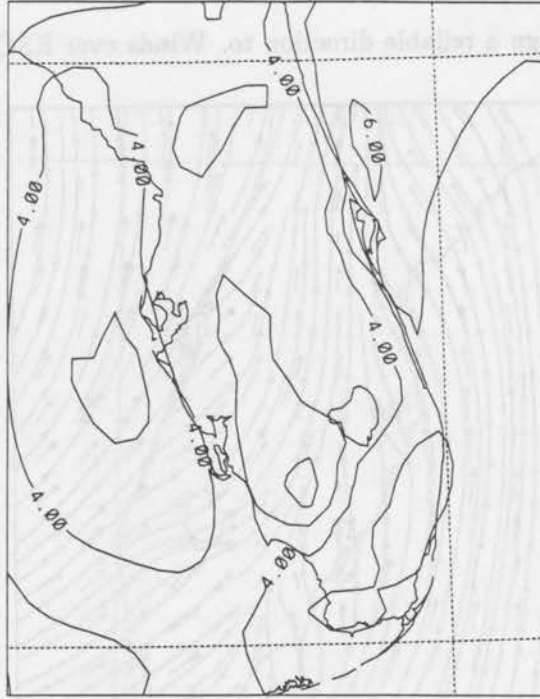


Figure 3.27: Near surface wind speeds (m/s); 21Z 29 July

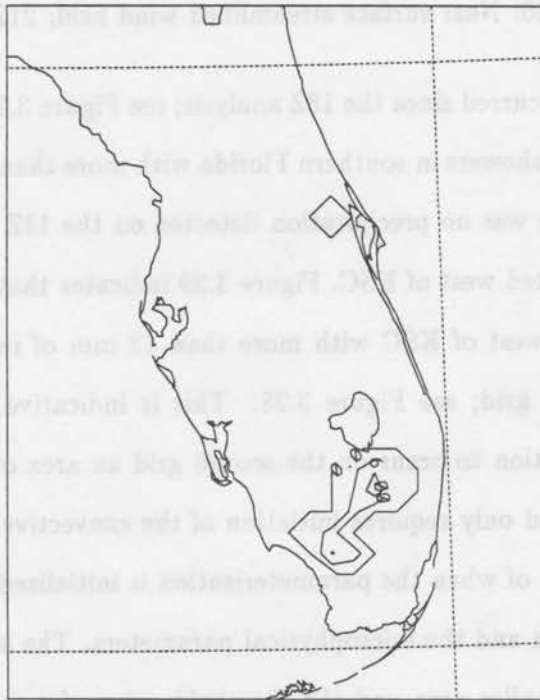


Figure 3.28: Accumulated convective precipitation (mm), contours = 6 mm, maximum contour = 12 mm; 21Z 29 July



Figure 3.29: Accumulated convective precipitation (mm), contour = 6 mm, maximum contour = 12 mm; 21Z 29 July

An analysis of the condensation mixing ratio indicates condensed water from model layer 2 through 22 (not shown). Figure 3.30 indicates the condensate mixing ratio at 48.6 m on grid 2 while Figure 3.31 is the same elevation for grid 3.

Undoubtedly most of the high values are due to rain and not strictly cloud water. Figure 3.30 and Figure 3.31 both indicate mixing ratios as high as 14 E-5 g/g , the majority of which is not liquid cloud water. The condensation ratio at model level 8 also indicates condensate and is not included but they are also as high as 39 E-5 g/g on Grid 3. The model also indicates condensate at an elevation of 7679 m on both the second and third grids; see Figures 3.32 and 3.33. The placement of the storm west of KSC agrees quite well with the 2135Z NMC radar summary; refer to Figure 3.34. The model depictions agree well between Grid 2 and Grid 3. The cloud coverage is slightly larger on Grid 2 but this is due to the issues relating to initiating convection on a grid addressed earlier.



Figure 3.30: Condensate mixing ratio (g/g), elevation = 48.6 m contour = 1 E-5 g/g, maximum contour = 14 E-5 g/g; 21Z 29 July

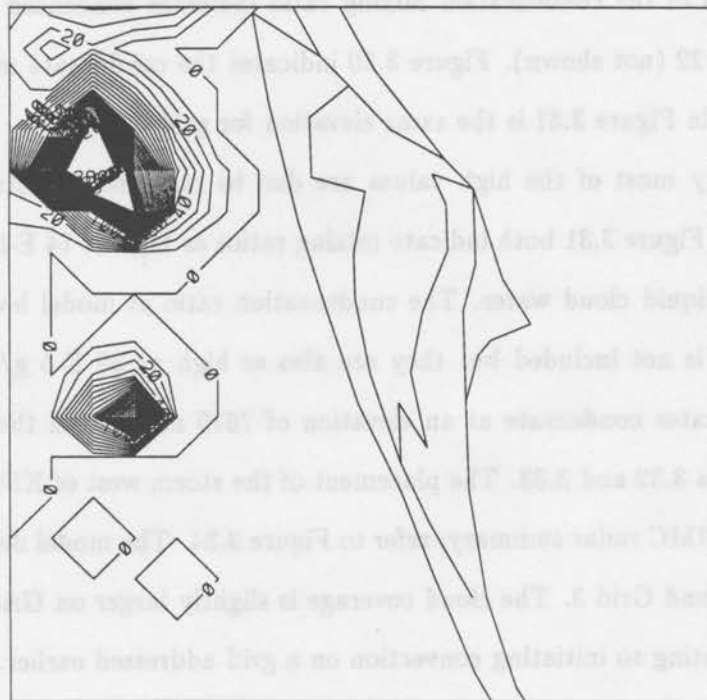


Figure 3.31: Condensate mixing ratio (g/g), elevation = 48.6 m contour = 1 E-5 g/g, maximum contour = 39 E-5 g/g; 21Z 29 July



Figure 3.32: Condensate mixing ratio (g/g), elevation = 7679 m, contour = 1 E-5 g/g, maximum contour = 32 E-5 g/g; 21Z 29 July

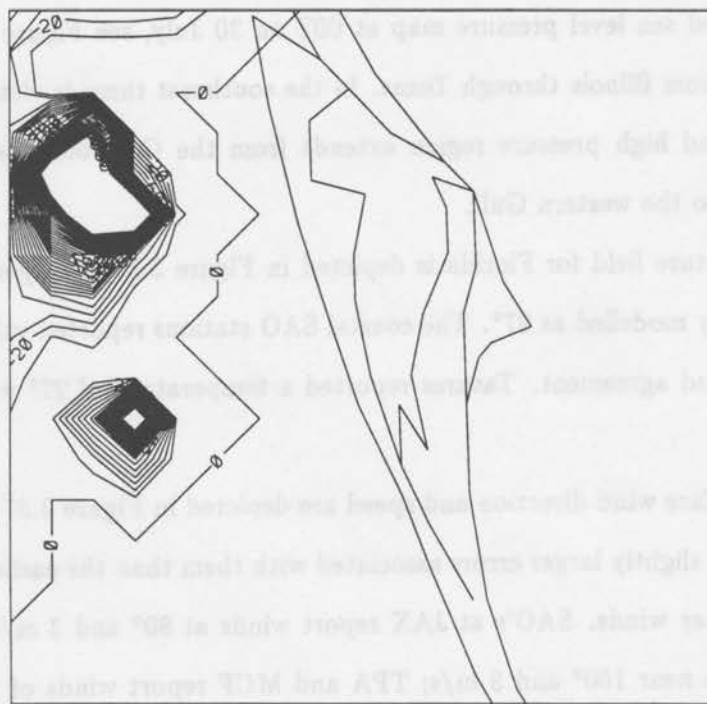


Figure 3.33: Condensate mixing ratio (g/g), elevation = 7679 m, contour = 1E-5 g/g, maximum contour = 39 E-5 g/g; 21Z 29 July

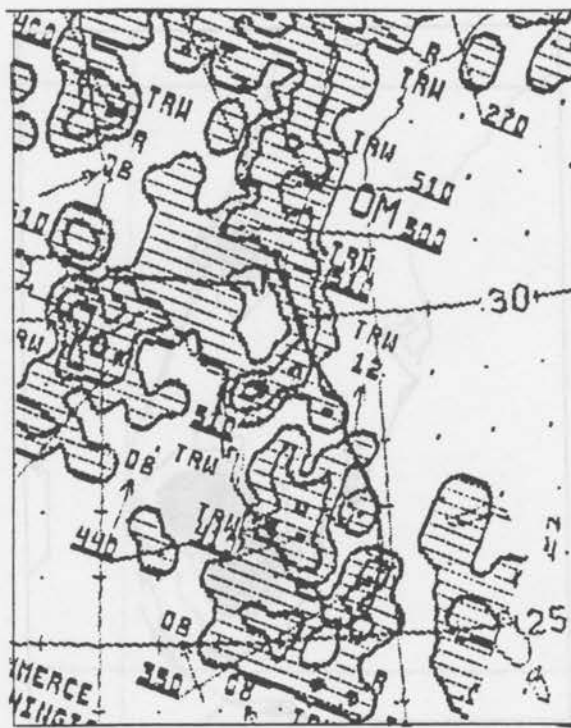


Figure 3.34: NMC radar summary; 2135Z 29 July

The 30 July 00Z Analysis

The predicted sea level pressure map at 00Z on 30 July, see Figure 3.35, indicates a front extending from Illinois through Texas. In the southeast there is virtually no pressure gradient. A broad high pressure region extends from the Caribbean across the Florida peninsula and into the western Gulf.

The temperature field for Florida is depicted in Figure 3.36. Temperatures along the coast are generally modelled as 27°. The coastal SAO stations reported values of 28° or 29° which is quite good agreement. Tavares reported a temperature of 27° which is the same as the model.

The near surface wind direction and speed are depicted in Figure 3.37 and Figure 3.38. These values have slightly larger errors associated with them than the earlier analyses. This is due to the lighter winds. SAO's at JAX report winds at 80° and 3 m/s; MIA and PBI both report winds near 160° and 3 m/s; TPA and MCF report winds of 260° and 3 m/s. Modeled winds agree very well with the speeds. Winds at Tavares are 300° and 2.5 m/s instead of 160° at 3 m/s. Tavares is near the center of the convergence zone though and

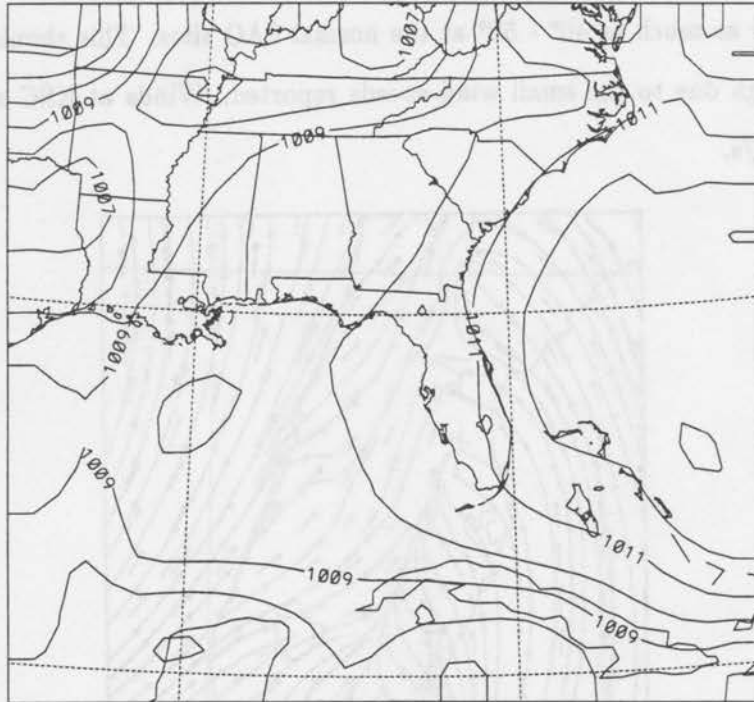


Figure 3.35: Mean sea level pressure (mb); 00Z 30 July

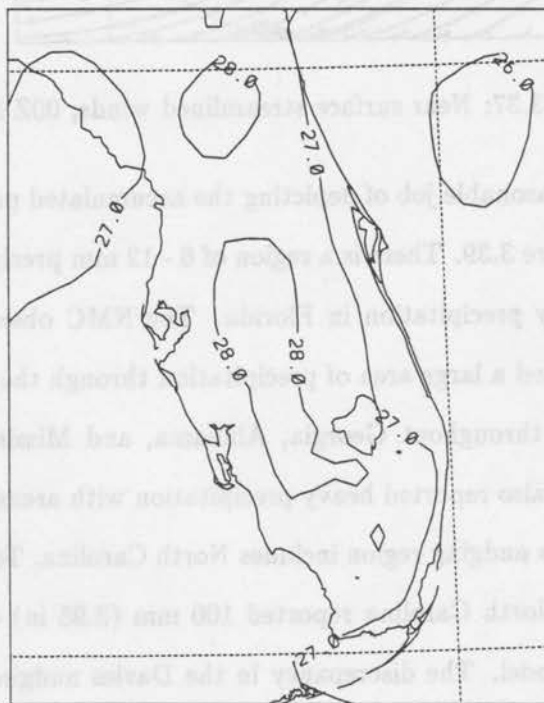


Figure 3.36: Temperature ($^{\circ}\text{C}$); 00Z 30 July

large changes in the wind direction can be expected on either side of the zone. The direction is different by as much as $40^\circ - 50^\circ$ at the normal SAO sites. This should not be a major concern though due to the small wind speeds reported. Winds at KSC are forecast to be 150° and 6 m/s.

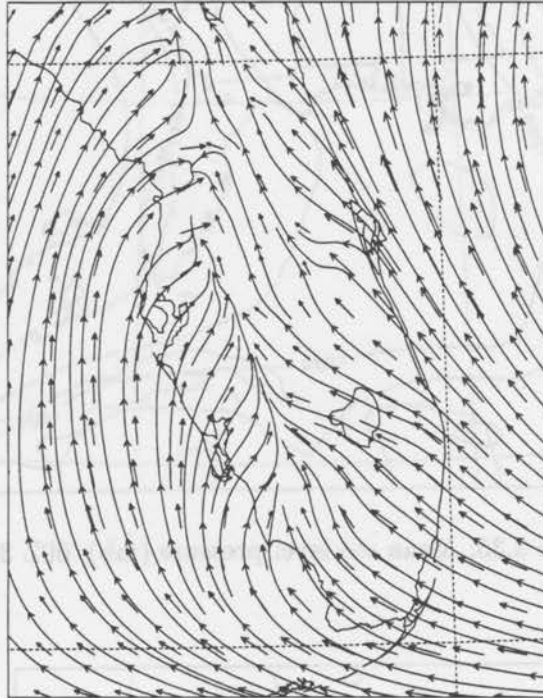


Figure 3.37: Near surface streamlined winds; 00Z 30 July

The model did a reasonable job of depicting the accumulated precipitation on the large grid in Florida, see Figure 3.39. There is a region of 6 - 12 mm precipitation in the southern Appalachians and heavy precipitation in Florida. The NMC observed precipitation map valid at 30 July 12Z noted a large area of precipitation through the Carolina's and an area of lighter precipitation throughout Georgia, Alabama, and Mississippi; see Figure 3.40. Several areas in Florida also reported heavy precipitation with areas of lighter precipitation interspersed. The Davies nudging region includes North Carolina, Tennessee, Arkansas, and Louisiana. Regions of North Carolina reported 100 mm (3.95 in) even though very little was predicted by the model. The discrepancy in the Davies nudging region should not be a major concern though since the data has been manipulated by the computer. There is a report of 48 mm (1.89 in) just north of KSC. The model forecast precipitation accumulations

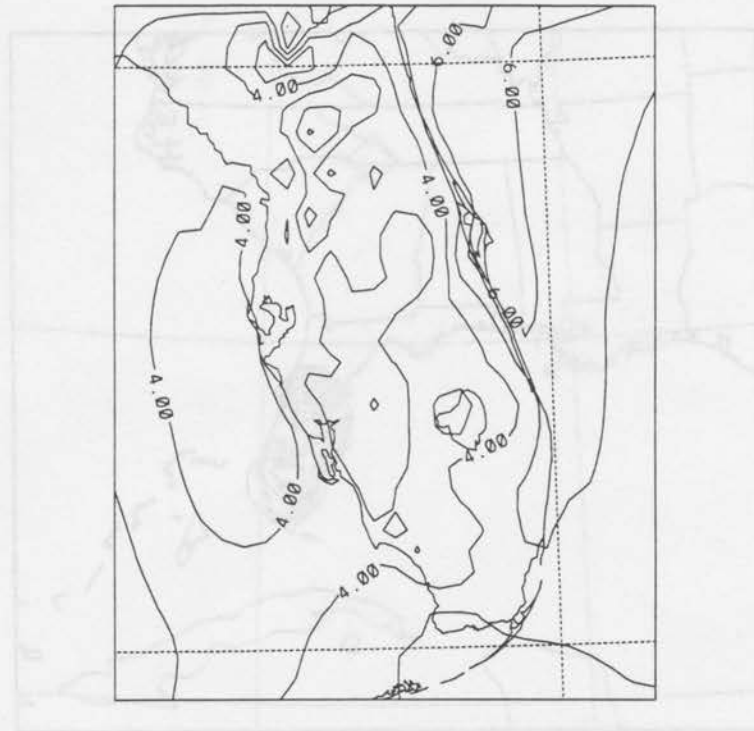


Figure 3.38: Near surface wind speeds (m/s); 00Z 30 July

between 24 - 30 mm (0.95 - 1.18 in) in Florida. These are very reasonable results given the 80 kilometer grid. The NGM was predicting 30 mm of accumulated precipitation during this period also.

The second grid indicated two areas of precipitation in Florida, one centered just west of KSC and another region south of Lake Okeechobee; see Figure 3.41. The region west of KSC had between 12 and 18 mm of precipitation. The southern area contains an area of between 18 and 24 mm of precipitation. The second grid has no precipitation on the west coast through central Florida. The NMC precipitation summary indicates that regions of the west Florida coast received approximately 1 mm (0.05 in) of precipitation. The lack of precipitation is related to the lack of clouds in western Florida noted in the 18Z discussion. While the lack of precipitation and clouds may be somewhat disconcerting this issue will be addressed in Chapter 5.

The third grid indicates a broad region west of KSC that receives up to 30 mm of precipitation, see Figure 3.42. This is in very good agreement with the data available from the CaPE experiment, see Table 3.1. Only 4 mm of precipitation is indicated at

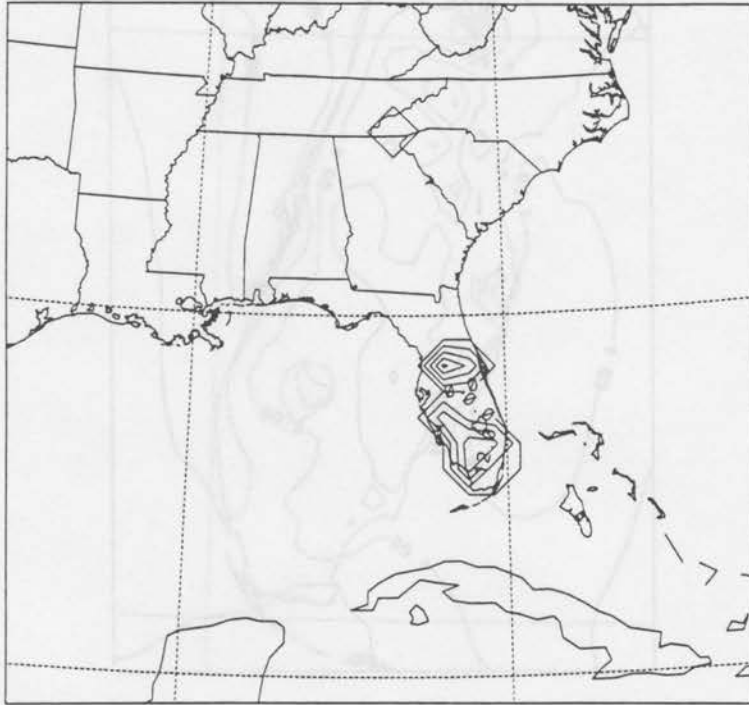


Figure 3.39: Accumulated convective precipitation (mm), contour = 6 mm, maximum contour = 24 mm; 00Z 30 July

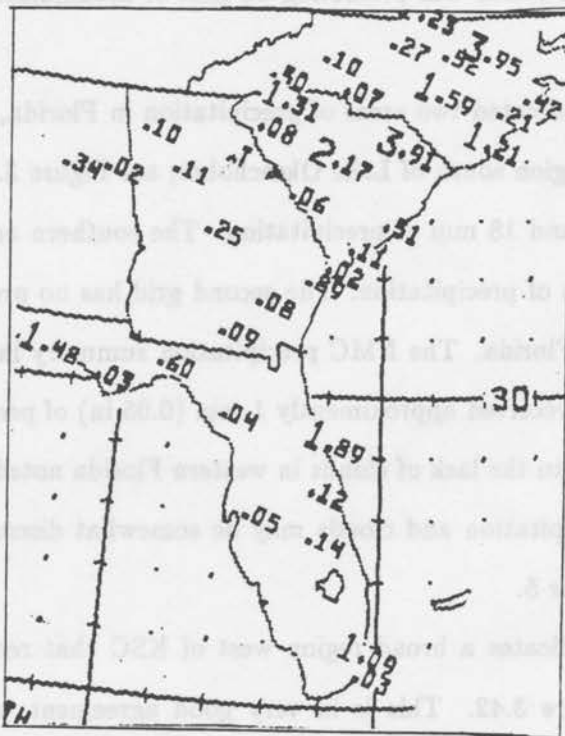


Figure 3.40: NMC precipitation summary (in); 12Z 30 July



Figure 3.41: Accumulated convective precipitation (mm), contour = 6 mm, maximum contour = 18 mm; 00Z 30 July

Cape Canaveral which is the barrier island where no precipitation was observed. Very sharp gradients are indicated from the data and the model. Titusville received 3 mm of precipitation while a location 10 kilometers west received 26 mm. Locations 40 kilometers south southwest of Titusville received 40 - 50 mm of precipitation but a rain gauge just 15 kilometers south of Titusville recorded only 9 mm. The NMC precipitation reports 48 mm of precipitation through 12Z 30 July; see Figure 3.39. This figure may be excessive for the present study which ends at 00Z on 30 July. The rain amounts agree well with the CaPE data which was collected during the valid period of the study. A rain gauge operated by USJRB did record 55 mm but the other gauges report amounts considerably less.

This illustrates one of the difficulties inherent in predicting precipitation. Precipitation is not a continuous field such as temperature or pressure. Because it rains at two locations 10 kilometers apart it does not imply that it rained between them. One of the difficulties of any analysis package such as the VAN package is that it only has data at discrete points and it does tend to smooth fields such as precipitation.

Table 3.1: CaPE Rainfall data

Site	Latitude	Longitude	Amount (mm)
USGS addison	28.53	80.82	9
USGS goat creek	27.94	80.60	4
USGS sebastian river	27.83	80.50	19
USJRB 111	27.70	80.58	25
USJRB 120	27.77	80.59	32
USJRB 124	27.89	80.67	2
USJRB 126	27.96	80.56	20
USJRB 128	27.95	80.61	9
USJRB 225	28.34	80.94	55
USJRB 265	28.21	80.92	41
USJRB 271	28.45	80.90	6
USJRB 294	28.62	80.96	26

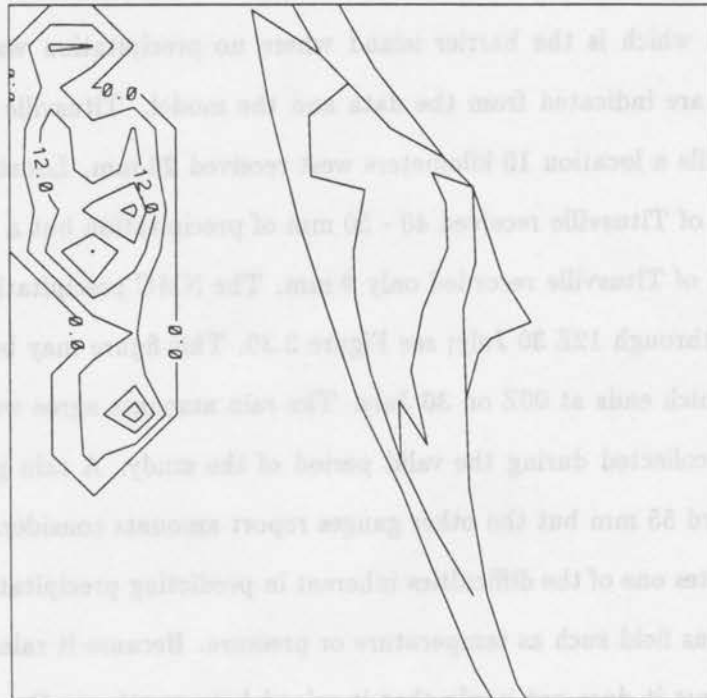


Figure 3.42: Accumulated convective precipitation (mm), contour = 6 mm, maximum contour = 24 mm; 00Z 30 July



Figure 3.43: NMC radar analysis; 0035Z 30 July

The upper air panels at 850 mb, 700 mb, 500 mb and 200 mb agree qualitatively with the observed geopotential fields; the model fields have lower geopotential heights though. Even though the field strengths are not identical the relative placement of the systems is quite excellent.

There are still several late afternoon thunderstorms in Florida as the Julian day comes to a close. Figure 3.43 shows large regions of condensate at the first model level. This pattern is continued at model levels represented at 907 m and 7679 m. The 0035Z radar summary from NMC indicates a line of thunderstorms to 15 kilometers (50000 feet) from central Florida to off the coast at Jacksonville; see Figure 3.43. The line appears to move through the area after the valid time of the study. Figure 3.44 provides a detailed view of the low level condensate threatening the Space Center. Notice the large region in the center corresponding to a mixing ratio of $39 \text{ E-}5 \text{ g/g}$.

3.4 Changing the radiation simulation

A RAMS simulation was also performed using the Mahrer/Pielke radiation scheme. As noted in Chapter 2 this radiation code neglects cloud reflection and short wave radiation.



Figure 3.44: Condensate mixing ratio (g/g), elevation = 48.6 m, contour = 1 E-5 g/g, maximum contour = 39 E-5; 00Z 30 July

For this discussion we will focus on the 12 hour forecast valid at 00Z on 30 July. In addition to changing the radiation scheme the threshold value for vertical velocity was changed on grid 3 from 0.1 to 0.08 m/s. This change will allow cloud formation and precipitation on Grid 3 to occur earlier than the best case described before.

Figure 3.45 depicts the sea level pressure analysis for Grid 1. The same general pattern is evident as in Figure 3.34, a weak pressure ridge is dominating Florida weather. Closer examination however reveals that the pressures are approximately 1 mb lower than the simulation using the Chen/Cotton radiation scheme.

Of more interest than the pressure is how the microphysical fields responded to changing the radiation. The accumulated precipitation field is vastly different from the previous simulation; see Figure 3.46. Precipitation was predicted along the Mississippi/Tennessee border and throughout much of the coastal and piedmont regions of North Carolina. The region just south of Charlotte is modelled as receiving 6 mm of precipitation while regions the southern North Carolina coast received 18 mm. As noted earlier this region has been manipulated by the Davies nudging scheme so the results are not meaningful. This radiation

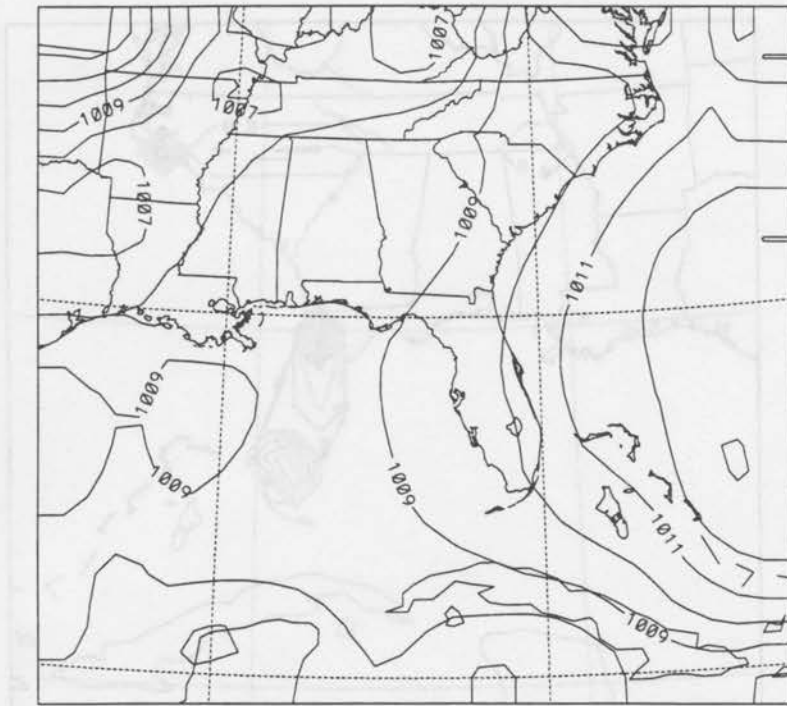


Figure 3.45: Mean sea level pressure (mb); 00Z 30 July

scheme does seem to form more precipitation than the Chen/Cotton scheme. There are also two distinct areas of precipitation in Florida. The northern maximum is located southwest of JAX and has 48 mm of precipitation, twice the amount previously simulated. Southern Florida has a maximum of 30 mm.

At 18Z no clouds were detected at model level 2 or 8 (48.6 m and 907 m, respectively). Clouds were detected at 7679 m on grid 2 but they were over Key West, not offshore from Miami. At 00Z 30 July condensate mixing ratios were detected at the second model level on grids 2 and 3. The analysis for Grid 3 is shown in Figure 3.47. This analysis agrees with the first simulation in that the clouds are in the southwest quadrant of the domain but these clouds are much drier. The maximum mixing ratio is $7 \text{ E-}5 \text{ g/g}$ compared to $39 \text{ E-}5 \text{ g/g}$ previously. Also recall that the current simulation has a lower vertical velocity threshold which allows it to produce clouds more readily.

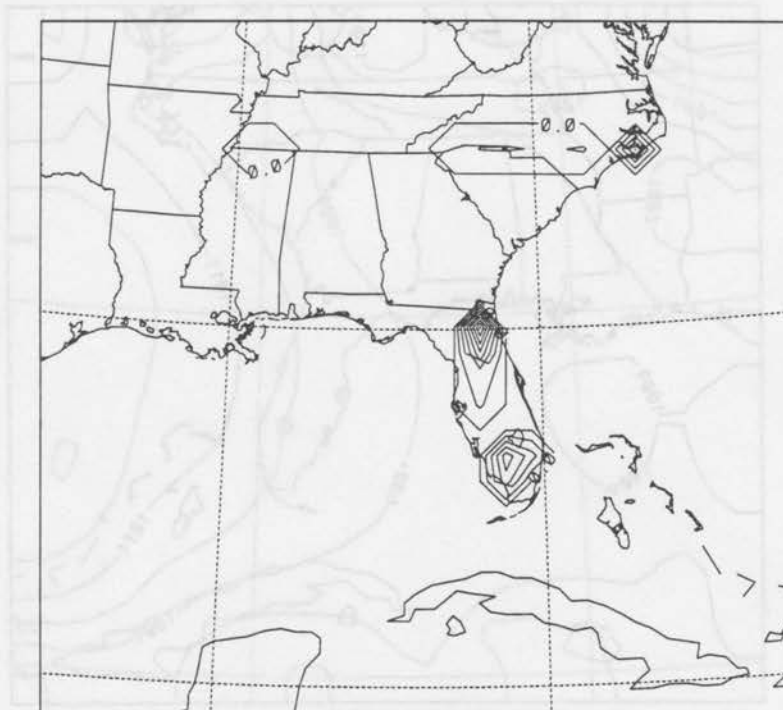


Figure 3.46: Accumulated convective precipitation (mm), contour = 6 mm, maximum contour = 48 mm; 00Z 30 July

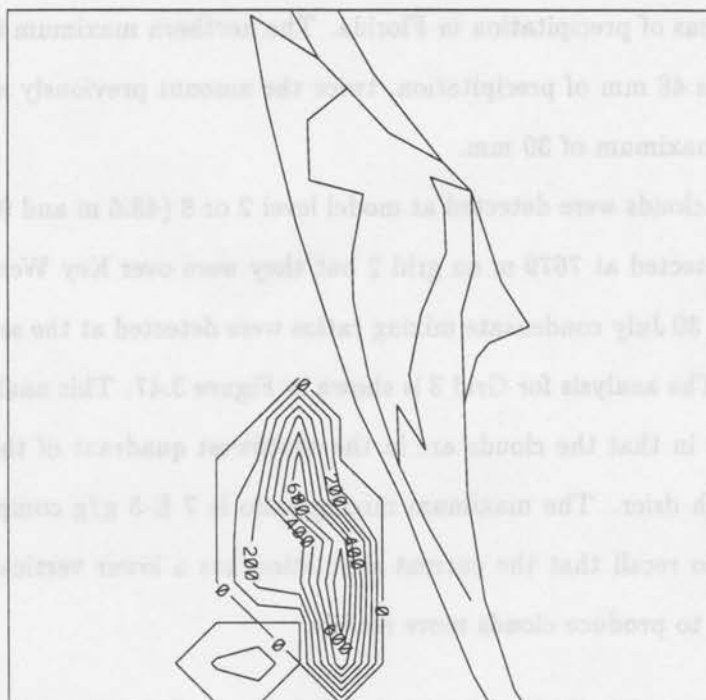


Figure 3.47: Mixing condensation ratio (g/g), elevation=48.6 m, contour = $1 \text{ E-}5 \text{ g/g}$, maximum contour = $7 \text{ E-}5 \text{ g/g}$; 00Z 30 July

Chapter 4

PRODUCING AN AVIATION FORECAST

4.1 Producing Terminal Aerodrome Forecasts

The first question to be solved when producing an aviation forecast is who are you forecasting for. This is not a trivial or absurd question. Aviation forecasts are designed on threshold values. The Federal Aviation Administration (FAA) is charged with producing forecasts for the general aviation community. The FAA has determined certain critical demarcations in the reported ceiling and visibility to be used to determine when instruments should be used to help aircraft land. Visual Flight Rules (VFR) require ceilings above 3000 feet and visibilities greater than 5 miles. Marginal Visual Flight Rules (MVFR) are less than VFR conditions but greater than 1000 foot ceilings and visibility greater than 3 miles. Instrument Flight Rules (IFR) require ceilings greater than 500 feet and visibilities greater than 1 mile. Low Instrument Flight Rules (LIFR) are required when the ceiling is less than 500 feet or the visibility is less than 1 mile. Notice that flight rules are based on the lower of the two criteria. It is possible to have ceilings of 800 feet (IFR) and visibilities of 0.5 miles which would require LIFR flight plans. This scenario is complicated because the United States Air Force and the Navy have different rules from each other and the FAA. Each airport can also establish criteria according to its needs for other requirements in the aviation forecast. For instance, there might be a rule that only pilots with more than 1000 hours can land if the ceiling is less than some threshold. This threshold would have to be added to those already established.

The parameters forecast for an aviation forecast include the minimum altimeter, wind direction and speed, turbulence, icing, cloud base and coverage, visibility, restrictions to visibility, thunderstorm occurrence. The minimum altimeter is defined as the lowest altimeter that is expected in the forecast period. All of the parameters have some tolerances

that allow for some variation between the observations and the forecast. However, if the discrepancy between the forecast and observations exceeds this tolerance then the forecast must be changed. Of the parameters needed in the aviation forecast perhaps the easiest to determine is the altimeter. As noted in Chapter 3 RAMS depicts the pressure field very accurately. It must be noted that there is a caution in using the pressure field forecast. If you examine the pressure field in Figure 3.2 there is an interesting discrepancy. The 12Z observations report the pressure as; MIA, 1017; PBI, 1017; JAX, 1016; TPA, 1016; Tallahassee 1015; Charleston, SC, 1016. All pressures are 3-4 mb higher than the simulation. This tendency continues throughout all the simulations examined at all times. The pressure analyzed for the model is the mean pressure at *48 meters AGL, not the surface*. This causes the modeled pressures to be several millibars lower than the surface pressure. Realizing that the reported pressure is high it is a simple matter to calculate the actual surface pressure using a hydrostatic integration.

RAMS also performs excellently in forecasting the winds near the surface. All models have a difficult time verifying the wind direction in the case of light winds (less than 5 m/s or 10 knots). FSL has avoided this problem by only verifying the direction when the speed is greater than 10 knots (Cairns et al., 1993). This seems to be a reasonable solution since it eliminates the wide variability in the direction that can render statistical verification meaningless. Also, most anemometers will not report a change of direction if the wind speed is less than 1.5 m/s. This can severely degrade any results when analyzing how well the model performs. Aviation forecasts are produced to aid pilots. Light winds do not pose a flight hazard under normal conditions. The area of concern is when the winds are high and especially if the wind is perpendicular to the runway. Abrupt changes in the wind direction may have an adverse impact on the approach pattern if the active runway is changed.

RAMS is capable of producing forecasts of icing and turbulence but these parameters were not addressed in this study. Both of these are assumed to occur in the presence of thunderstorms. For more information the reader is directed to Cairns et al. (1993). FSL is producing yes/no forecasts of both parameters and is also constructing soundings that allow for analyses every 1000 feet to aid in the forecasting of these flight hazards.

With these parameters forecasts the question remains of forecasting clouds, visibility and the occurrence of thunderstorms. These parameters are intimately related, especially in precipitation events. A thunderstorm will lower the ceiling and reduce visibility. It is not uncommon for thunderstorms in Florida to reduce the ceiling to several hundred feet and reduce the visibility to less than a half mile, 800 meters. As noted in Chapter 3, RAMS will explicitly forecast the presence of cloud water and several other microphysical species. This was used to determine the presence of clouds in these simulations. The vertical level structure of the model may be constructed to aid in the forecast. For instance, I was primarily interested in two extremes of flying; when ceilings are below 200 feet or above 3000 feet. Because of these interest I chose to analyze the data at 48.6 m (160 feet) and 907 m (2977 feet). RAMS is an extremely versatile forecasting tool with many options that can aid in producing a forecast. The individual vertical levels may be specified instead of specifying an initial spacing and a stretching factor. This would allow each agency to specify levels it deems critical and produce forecasts at those levels. For instance, the FAA models could produce forecasts at 500, 1000, and 3000 feet because those are critical levels. Care must be taken though not to introduce numerical instabilities into the model due to poor choices of vertical levels and spacings.

A second problem to be addressed is what constitutes a cloud. RAMS currently predicts the presence of cloud water but not areal coverage. The categories for cloud coverage are clear, scattered, broken and overcast. Clear implies less than 10 percent areal coverage by clouds. Scattered is defined by areal coverage between 10 percent and 50 percent. Broken is more than 50 percent and is considered the ceiling. Overcast is greater than 90 percent coverage. Some information can be obtained from the model analysis but there is currently no code to determine fractional cloud coverage. The height of a ceiling is crucial to aviation forecasting. An additional concern is that the coverage is cumulative as seen from the surface. If there is a layer of clouds covering 30 percent at 1000 m and another layer covering 30 percent at 3000 m there may or may not be a ceiling. If the clouds overlap it is possible that there is only 30 percent total cloud coverage. The other extreme is that the cloud layers do not overlap. In this case the total coverage is 60 percent and the ceiling is at 3000 m.

I have also compared detecting clouds by horizontal cross sections versus vertical cross sections. Each of these tools have their advantages. Earlier the horizontal cross sections were analyzed. These plots covered a large area at critical heights to determine the presence of clouds. The detection of thunderstorms required the analysis of several different altitudes to determine the vertical extent of a cloud.

By contrast, the vertical cross section allows for the instant determination of depth of a cloud or storm system. Analyses such as Figures 4.1 and 4.2 can be extremely useful in determining cloud base and height. For instance, thunderstorm tops could be determined easily. The top of the thunderstorms depicted is approximately 16000 m (52000 feet). This agrees extremely well with the NMC radar summary at 2135Z (see Figure 3.34) which indicates thunderstorm tops of the same altitude. Figure 4.1 is an east-west cross section while Figure 4.2 is north-south. Notice the anvil region on Figure 4.2.

The difficulty is in choosing which coordinates to perform the cross section on. Cross sections performed by the VAN package hold either the x or y ordinate constant. Determining which cross section to analyze can be difficult though and is largely a matter of trial and error and this is best done interactively. Vertical cross sections can also be used to determine if there are any clouds at flight level and the maximum thunderstorms tops that can be expected. This could be beneficial for pilots who have to avoid clouds or those pilots who prefer to fly in them.

The last parameter to be included in an aviation forecast is the visibility and obstruction to visibility. Currently work is being done to include this parameter in RAMS but it is not yet available. Of the aviation parameters these might be the most difficult to forecast. The MAPS system used by FSL uses very simple algorithms to predict both visibility and obstruction to visibility (Cairns and Miller, 1993), but it is one of a few models that do forecast these variables. Part of the problem is the scale of visibilities and the need for detailed optical properties of the phenomena obstructing the visibility. It is not uncommon for the visibility to be reduced to less than a quarter mile in thunderstorms in the southeast. On the other hand observations in the west may have visibilities of 20 miles and light drizzle. Both of these observations have an obstruction to visibility but the range of visibility is quite large. A second problem is one of resolution. At distances less than 8000 m (5 miles),

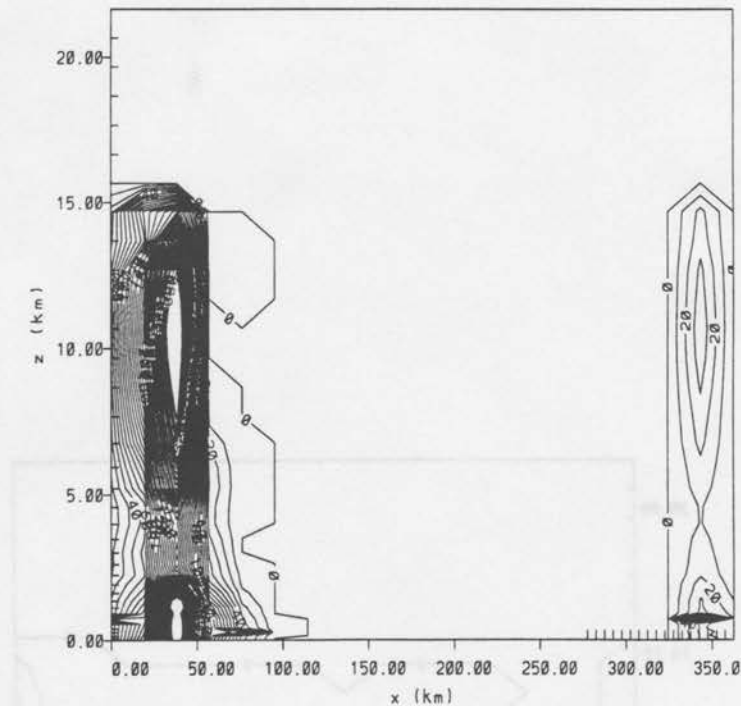


Figure 4.1: Condensation mixing ratio cross section (g/g), contour = $1 \text{ E-}5 \text{ g/g}$, maximum contour = 39 g/g ; 21Z 29 July

MVFR flight conditions, the visibility needs to be resolved at approximately 1600 m (1 mile) intervals. When visibilities are below 1600 m (1 mile), then the *resolution* should be on the order of 400 meters (one-quarter mile).

The forecast valid from 12Z 29 July to 00Z 30 July developed using the RAMS output is:

At 12Z: Wind direction 180° speed 1.5 m/s
 minimum pressure 1011 mb

Changing between 17-18Z: Wind direction 130° speed 3 m/s

Clouds: Scattered 400 m

Minimum pressure 1011 mb

Temporary conditions between 20-00Z:

Clouds: Broken 50 m Overcast 400 m.

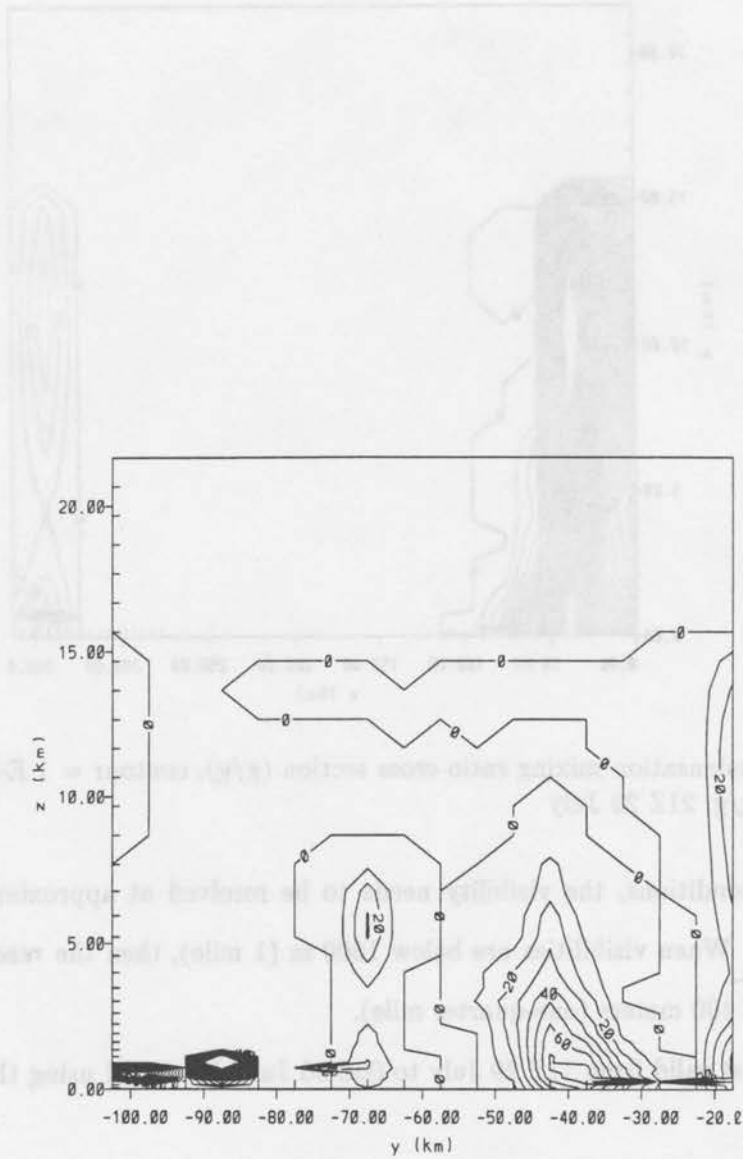


Figure 4.2: Condensation mixing ratio (g/g), contour = $1E-5$ g/g, maximum contour = $39 E-5$ g/g; 21Z 29 July

Chapter 5

CONCLUSIONS

It is both possible and practical to produce aviation forecasts with the aid of RAMS. RAMS may be used as a regional model and in many ways is far superior to the products issued by NMC currently in use in forecast offices throughout the country. The largest advantages are in the model resolution and versatility of RAMS. As noted earlier the resolution of the NGM is 320 kilometers. The 20 kilometer grid, Grid 2, used in this study has the capability to resolve features on the order of 80 kilometers.

The versatility of RAMS is also a positive factor in using it to aid forecasters. This versatility has a wide spectrum of possibilities; in the initialization of the model many different data sets may be used. In the actual model the vertical levels may be specified at altitudes that the user determines are critical, not just convenient. The placement and spacing of the horizontal grid may also be optimized by the user. The ISAN package may also be optimized to site specific criteria. This would include choosing the cross sections and parameters that are most important to that site. For instance, the error in temperature for aviation forecast can be several degrees with little effect. In this case the station may want to produce regional output similar to Figure 3.19 (Grid 2) instead of very local analysis similar to Figure 3.20 (Grid 3).

Currently RAMS can predict sea level pressure, wind speed and direction, icing, turbulence, cloud base and top, and the occurrence of thunderstorms. These are seven of the ten parameters required in aviation forecast. Work is continuing on the others and will be the topic of Chapter 6.

Chapter 6

FUTURE RESEARCH

The use of mesoscale models for numerical weather prediction is a relatively young field. The proposition that you can use one to produce an aviation forecast is still in its infancy. The areas of future research are divided into two different but related areas. The first is in mesoscale models in general and the second is topics for RAMS.

6.1 Mesoscale models

There is a very old and unattributable saying that says what you get out is only as good as what you put in or "garbage in, garbage out". This is true even of atmospheric models. Remember that Richardson's early attempts at numerical weather prediction were aborted due to the belief that the observations were bad. One of the areas that all models need to improve is in the initial data assimilation. The MAPS data set is an excellent choice for data if it is available. One area of future research is how to interface to different data sets having the same parameters. One such example would be interfacing the MAPS and ETA data sets. This would allow models to use the MAPS data over the US where it is available but use the ETA data over the ocean where MAPS is not available.

Another area of concern in modeling is in accurately predicting the water vapor flux at the surface. On land this is determined primarily by land use and vegetation type. There needs to be a standard file system that can be accessed similar to the topography files. Additionally, sea surface temperatures need to be made available in real time to determine the fluxes over the oceans. Peter Webster has also noted that the sea surface moisture flux is dependent on the salinity (private conversation). Future models may also require real time salinity measurements if extremely accurate atmospheric models are needed.

Transportability of models is also a concern throughout the community. Penn State and Colorado State both pride themselves on having the ability to model anywhere in the world by changing the latitude and longitude of their model domain (Warner and Seaman, 1990). It is not as easy as changing the latitude and longitude though. There are a host of variables that change with location. A set of climatological data or best first guesses should be determined for different regions of the world. For instance, the 2.5w parameterization scheme requires input of the maximum planetary boundary height. Most locations in the United States 1000 meters is probably a good approximation but modelers also need need values in London, Riyadh, or even Denver. Among the values that should have suggested values are the updraft velocities, cloud condensation nuclei spectrum, tropopause height, and the microphysical parameters; type, size, and concentration.

6.2 RAMS

RAMS in general is a living breathing entity with many continuous upgrades to its code being continually performed. One of the areas that is related to the above discussion is improving the model initialization. The model is already initialized from the MAPS data, what is needed is a way to fill the oceanic data voids with NGM, ETA or MRF data. Also, access should be attempted to the National Oceanic and Atmospheric Administrations sea surface temperature analysis. The analysis is on a 14 kilometer grid (Warner and Seaman, 1990) and is a vast improvement over the climatological data base currently in use. Work is currently under way to allow variable vegetation cover without having to perform this task manually. These files should probably be seasonal since the fluxes change rapidly depending on whether the plants are growing. There also needs to be a urban code added to the options. Temperatures and fluxes vary widely in major metropolitan areas such as Miami or Atlanta and will need to be accounted for.

The other major advances in RAMS can be made in the VAN package. As mentioned before methods must be developed to determine cloud base and coverage along with visibility and obstructions. The determination of cloud base is critical for aviation forecasts. Care must be taken to use the actual station elevation and not the model elevation. While this should not be a great concern in Florida there can be great discrepancies between the actual

station elevation and the model station elevation in mountainous regions. For instance, if the model is forecasting a cloud layer 100 m above the model surface and the actual station elevation is 100 m higher than the model surface the cloud base is now on the surface and not above ground. Another improvement to the VAN package is to output the altimeter setting. RAMS currently calculates the station pressure which can easily be converted to an altimeter setting. As the code currently is, the system can be a great benefit to forecasters but that information must be conveyed to the forecaster. This information exchange is conducted through the VAN package.

Currently the moisture variable is the mixing ratio of the various microphysical species. While they convey information about the model it is not in a form that most forecasters can understand. There is a great deal of difference between the statement that the vapor mixing ratio is 20 g/kg and the statement that the dew point is 25 °C (77 °F) at 1000 mb. All of these statements are equally as valid but a forecaster is more likely to understand a dew point instead of a mixing ratio.

Ultimately, RAMS will be located in a forecast office where it is unlikely that everyone will have an advanced degree in meteorology. This is the customer that the will pass judgment on suitability of RAMS and the ease at which it produces meaningful forecast products. The system employed must be extremely user friendly. A turn key version of RAMS with a recommended model parameters, activation of grids, and an interactive VAN package. This version does not necessarily need all the options that the research version of RAMS has.

Chapter 7

REFERENCES

- Anthes, Richard A. 1977: A Cumulus Parameterization Scheme Utilizing a One-Dimensional Cloud Model. *Mon. Wea. Rev.*, **105**, 270-286.
- , Daniel Keyser. 1979: Tests of a Fine-Mesh Model over Europe and the United States. *Mon. Wea. Rev.*, **107**, 963-984.
- . 1983: Regional Models of the Atmosphere in the Middle Latitudes. *Mon. Wea. Rev.*, **111**, 1306-1334.
- Betts, A.K., 1975: Parametric interperation of trade-wind cumulus budget studies. *J. Atmos. Sci.*, **32**, 1934-1945.
- Bougeault, Phillipe. 1985: A simple Parameterization of the Large-Scale Effects of Cumulus Convection. *Mon. Wea. Rev.*, **113**, 2108-2121.
- Cairns, Mary M, and Ronald J. Miller, 1993: *Verification Program Plan for Excercise 2*. National Oceanic and Atmospheric Administration, Environmental Research Laboratories, Forecast Systems Laboratory, Boulder, CO.
- and —, Steven C. Albers, Daniel L. Birkenheur, Brian D. Jamison, Craig S. Hartlough, Jennifer L. Mahoney, Adrian Marroquin, Paula T. McCaslin, James E. Ramer, Jerome M. Schmidt. 1993: *NOAA Technical Memorandum ERL FSL-5*. National Oceanic and Atmospheric Administration, Environmental Research Laboratories, Forecast Systems Laboratory, Boulder, CO.
- Chen, C. and W.R. Cotton. 1983: A one-dimensional simulation of the stratocumulus-capped mixed layer. *J. Appl. Meteor.*, **13**, 289-297.

- and —. 1987: The physics of the marine stratocumulus-capped mixed layer. *J. Atmos. Sci.*, **44**, 2951-2977.
- Cotton, William R., Roger A. Pielke, Patrick T. Gannon. 1976: Numerical Experiments on the Influence of the Mesoscale Circulation on the Cumulus Scale. *J. Atmos. Sci.*, **33**, 252-261.
- , M.A. Stevens, T. Nehr Korn, G.J. Tripoli. 1982: The Colorado State University three-dimensional cloud/mesoscale model - 1982. Part II: An ice phase parameterization. *J. de Rech. Atmos.*, **16**, 295-320.
- , G.J. Tripoli, R.M. Bauber, and E.A. Mulvihill, 1986: Numerical simulation of the effects of varying ice nucleation rates and aggregation processes on orographic snowfall. *J. Climate Appl. Meteor.* **25**, 1658-1680.
- , Gregory Thompson, Paul W. Mielke, Jr. 1993: Realtime Mesoscale Prediction on Workstations. Submitted to *Bull. Amer. Meteor. Soc.*.
- , G.J. Tripoli, R.M. Rauber. 1986: Numerical simulation of the effects of varying ice crystal nucleation rates and aggregation processes on orographic snowfall. *J. Appl. Meteor.*, **25**, 1658-1680.
- Cram, J.M. 1990: Numerical simulation and analysis of the propagation of prefrontal squall line. Ph.D. dissertation. Dept. of Atmo. Sci., Colorado State University, Fort Collins, CO 80523. 330 pp.
- Droegemeier, Kelvin K, Robert B. Wilhelmson. 1987: Numerical Simulation of Thunderstorm Outflow Dynamics, Part I: Outflow Sensitivity Experiments and Turbulence Dynamics. *J Atmos Sci*, **44**, 1180-1210.
- Flatau, P.J., G.J. Tripoli, J. Verlinde, and W.R. Cotton. 1989: The CSU-RAMS cloud microphysics module: General theory and code documentation. Technical Report 451, Colorado State University, Fort Collins, CO 80523.
- Frank, William M. 1983: The Cumulus Parameterization Problem. *Mon. Wea. Rev.*, **111**, 1859-1871.

- Fugita, T. T., 1981: Tornadoes and downburst in the context of generalized planetary scales. *J. Atmos. Sci.*, **38**, 1512-1534.
- , 1986: Mesoscale Classifications: Their History and Their Application to Forecasting. *Mesoscale Meteorology and Forecasting*, Peter Ray, ed., American Meteorological Society, Boston, 18-35.
- Golding, B.W. 1990: The Meteorological Office mesoscale model. *Meteorol. Mag.*, **119**, 81-96.
- . 1992: An Efficient Non-Hydrostatic Forecast Model. *Meteorology and Atmospheric Physics*, **50**, 89-103.
- Goose, Mother, 1986: *The Real Mother Goose*, Rand McNally and Company, Chicago, IL. p 37.
- Heckman, S.T. 1991: Numerical simulation of cirrus clouds - FIRE case study and sensitivity analysis. Masters thesis, Atmos. Sci. Paper No. 483, Colorado State University, Fort Collins, CO 80523. 132 pp.
- Hoke, James E., Norman A Phillips, Geoffrey J DiMego, Joseph G. Sela. 1989: The Regional Analysis and Forecast System of the National Meteorological Center. *Wea. and Fore.*, **4**, 323-334.
- Holton, James R. 1979: *An Introduction to Dynamical Meteorology*, Second Edition, Academic Press, Inc, New York, p 173-175.
- Job, The Book of. *The Holy Bible, New International Version*. Zondervan Bible Publishers, Grand Rapids MI, p 396-397.
- Junker, Norman W., James E. Hoke and Richard H. Grumm. 1989: Performance of NMC's Regional Models. *Wea. and Fore.*, **4**, 368-390.
- Kanamitsu, M., 1975: *On numerical prediction over a global tropical belt*. PhD thesis, Florida State University, Department of Meteorology, Tallahassee FL 32304.
- Klemp, J.B. and D.R. Durran. 1983: An upper boundary condition permitting internal gravity wave radiation in numerical mesoscale models. *Mon. Wea. Rev.*, **111**, 430-444.

- and R.B. Wilhelmson. 1978a: The simulation of three-dimensional convective storm dynamics. *J. Atmos. Sci.*, **35**, 1070-1096.
- and —. 1978b: Simulations of right- and left-moving storms produced through storm splitting. *J. Atmos. Sci.*, **35**, 1097-1110.
- Krishnamurti, T.N., M. Kanamitsu, R. Godbole, C.B. Chang, F. Carr, and J. Chow, 1976: Study of monsoon depression (II), Dynamical structure. *J. Meteor. Soc. Japan.* **54**, 208-225.
- Kuo, H.L. 1974: Further Studies of the Parameterization of the Influence of Cumulus Convection on the Large-Scale Flow. *J. Atmos. Sci.*, **31**, 1232-1240.
- Lilly, D.K. 1962: On the numerical simulation of bouyant convection. *Tellus*, **XIV**, 148-172.
- Louis, J.F. 1979: A parametric model of vertical eddy fluxes in the atmosphere. *Boundary-layer Meteorol.*, **17**, 187-202.
- Mahrer, Y., R.A. Pielke. 1977: A numerical study of the airflow over irregular terrain. *Beitrage zur Physik der Atmosphere*, **50**, 98-113.
- Nicholls, Melvin E., Roger A. Peilke, Joseph L. Eastman, Cathy A. Finley, Walter A. Lyons, Craig J. Tremback, Robert L. Walko, and William R. Cotton, 1993: Applications of the numerical model to dispersion over urban areas. *The effect of urbanisation on windfields, air pollution spreading and wind forces*, NATO Advanced Study Institute.
- Orlanski, I. 1975: A Rational subdivision of scales for atmospheric processes. *Bull. Amer. Meteor. Soc.*, **56**, 527-530.
- Pielke, R.A., W.R. Cotton, R.L. Walko, C.J. Tremback, W.A. Lyons, L.D. Grasso, M.E. Nicholls, M.D. Moran, D.A. Wesley, T.J. Lee and J.H. Copeland. 1992: A Comprehensive Meteorological modeling System - RAMS. *Meteorology and Atmospheric Physics*, **49**, 69-91.

- , Ytzhag Mahrer. 1978: Verification Analysis of the University of Virginia Three-Dimensional Mesoscale Model Prediction over South Florida for 1 July 1973. *Mon. Wea. Rev.*, **106**, 1568-1589.
- Thompson, Gregory, 1993: Prototype real-time mesoscale prediction during 1991-1992 winter season and statistical verification of model data. M.S. thesis. Atmos. Sci. Paper 521. Department of Atmospheric Science, Colorado State University, Fort Collins, CO 80523.
- Thompson, Philip D., Robert O'Brien. 1965: *Weather*, Time Life Books, Time Incorporated, New York, p 58.
- Tremback, C.J. 1990: Numerical simulation of a mesoscale convective complex: model development and numerical results. Ph.D. dissertation. Atmos. Sci. Paper No. 465, Department of Atmospheric Science, Colorado State University, Fort Collins, CO 80523, 247 pp.
- and R. Kessler. 1985: A surface temperature and moisture parameterization for use in mesoscale numerical models. Preprint volume of the Seventh Conference on Numerical Weather Prediction, June 1985, AMS, Montreal, Canada, 355-358.
- , G. Tripoli, R. Arritt, W.R. Cotton, R.A. Pielke. 1986: The Regional Atmospheric Modeling System. Proceedings of the International Conference on Development and Application of Computer Techniques to Environmental Studies, Los Angeles, CA. 601-607.
- Tripoli, G.J. 1986: A numerical investigation of an orogenic mesoscale convective system. Ph.D. dissertation. Atmos. Sci. Paper No. 401, Dept. of Atmos. Sci., Colorado State University, Fort Collins, CO 80523, 290 pp.
- and W.R. Cotton. 1980: A numerical investigation of several factors contributing to the observed variable intensity of deep convection over South Florida. *J. Appl. Meteor.*, **19**, 1037-1063.

—, and —. 1982: The Colorado State University three-dimensional cloud/mesoscale model - 1982. Part I: General theoretical framework and sensitivity experiments. *J. de Rech. Atmos.*, **16**, 185-220.

Walko, R. and C. Tremback, 1992: *The RAMS users guide*, Colorado State University, Ft Collins, CO 80523.

Warner, Thomas T., Nelson L. Seaman. 1990: A Real-Time, Mesoscale Numerical Weather-Prediction System Used for Research, Teaching, and Public Service at the Pennsylvania State University. *Bull. Amer. Meteo. Soc.*, **71**, 792-805.

Weissbluth, Micheal J. 1991: Convective Parameterization in Mesoscale Models. Ph.D. dissertation. Atmos. Sci. Paper No. 486. Dep. of Atmos. Sci., Colorado State University, Fort Collins, CO 80523. 211 pp.

—, and William R. Cotton. 1993: The Representation of Convection in Mesoscale Models. Part I: Scheme Fabrication and Calibration. Submitted to *J. Atmos. Sci.*.

X18-5
~~71311~~
 2